The bending vibrational levels of the acetylene cation: A case study of the Renner-Teller effect in a molecule with two degenerate bending vibrations

Sheunn-Jiun Tang, Yung-Ching Chou, Jim Jr-Min Lin, and Yen-Chu Hsu

Citation: The Journal of Chemical Physics **125**, 133201 (2006); doi: 10.1063/1.2199827
View online: http://dx.doi.org/10.1063/1.2199827
View Table of Contents: http://scitation.aip.org/content/aip/journal/jcp/125/13?ver=pdfcov
Published by the AIP Publishing

The bending vibrational levels of the acetylene cation: A case study of the Renner-Teller effect in a molecule with two degenerate bending vibrations

Sheunn-Jiun Tang,[a] Yung-Ching Chou, Jim Jr-Min Lin,[b] and Yen-Chu Hsu[c]
Institute of Atomic and Molecular Sciences, Academia Sinica, P. O. Box 23-166, Taipei 10617, Taiwan, Republic of China

(Received 20 February 2006; accepted 4 April 2006; published online 2 October 2006)

Forty three vibronic levels of $C_2H_2^+$, $\tilde{X}\,^2\Pi_u$, with $v_4=0-6$, $v_5=0-3$, and $K=0-4$, lying at energies of 0–3520 cm^{-1} above the zero-point level, have been recorded at rotational resolution. These levels were observed by double resonance, using $1+1'$ two-color pulsed-field ionization zero-kinetic-energy photoelectron spectroscopy. The intermediate states were single rovibrational levels chosen from the $\tilde{A}\,^1A_u$, $4\nu_3$ ($K=1-2$), $5\nu_3$ ($K=1$), $\nu_2+4\nu_3$ ($K=0$), and 47 206 cm^{-1} ($K=1$) levels of C_2H_2. Seven of the *trans*-bending levels of $C_2H_2^+$ ($v_4=0-3$, $K=0-2$) had been reported previously by Pratt *et al.* [J. Chem. Phys. **99**, 6233 (1993)]; our results for these levels agree well with theirs. A full analysis has been carried out, including the Renner-Teller effect and the vibrational anharmonicity for both the *trans*- and *cis*-bending vibrations. The rotational structure of the lowest 16 vibronic levels (consisting of the complete set of levels with $v_4+v_5\leqslant 2$, except for the unobserved upper $^2\Pi_u$ component of the $2\nu_4$ overtone) could be fitted by least squares using 16 parameters to give an rms deviation of 0.21 cm^{-1}. The vibronic coupling parameter ε_5 (about whose magnitude there has been controversy) was determined to be -0.0273_7. For the higher vibronic levels, an additional parameter, r_{45}, was needed to allow for the Darling-Dennison resonance between the two bending manifolds. Almost all the observed levels of the $v_4+v_5=3$ and 4 polyads (about half of the predicted number) could then be assigned. In a final fit to 39 vibronic levels with $v_4+v_5\leqslant 5$, an rms deviation of 0.34 cm^{-1} was obtained using 20 parameters. An interesting finding is that Hund's spin-coupling cases (a) and (b) both occur in the Σ_u components of the $\nu_4+2\nu_5$ combination level. The ionization potential of C_2H_2 (from the lowest rotational level of the ground state to the lowest rotational level of the cation) is found to be 91 953.77±0.09 cm^{-1} (3σ). © *2006 American Institute of Physics*. [DOI: 10.1063/1.2199827]

I. INTRODUCTION

The properties of the acetylene cation have long been of interest in both mode-selected ion-molecule reactions and interstellar chemistry.[1–6] Although the photoelectron spectrum of C_2H_2 was first recorded in 1967,[7] no high resolution work on the cation was done until 1987, when Jagod *et al.*[6] analyzed the ν_3 fundamental of the $^2\Pi_u$ ground state of $C_2H_2^+$ at 3135.981 cm^{-1}. More recent photoelectron spectroscopy[8,9] has given values for ν_1 and ν_2 (3307 and 1829 cm^{-1}, respectively), but controversy has surrounded the bending modes. The first estimate of ν_4 was made by Reutt *et al.*[8] using photoelectron spectroscopy; with the help of deuterium substitution they obtained a value of 837 cm^{-1}. Later, Pratt *et al.*[10] employed $1+1'$ two-color zero-kinetic-energy (ZEKE) photoelectron spectroscopy via the *trans*-bent $\tilde{A}$ state of acetylene; this gave an unambiguous value of 694 cm^{-1}, with the vibronic coupling parameter ε_4 equal to 0.30. They also tentatively assigned a feature at 748 cm^{-1} to ν_5.

The structures of the bending levels of the acetylene cation are complicated by interaction with the orbital angular momentum in the $\tilde{X}\,^2\Pi_u$ state (Renner-Teller effect). This effect has been studied extensively in tri-atomic molecules, both theoretically[11–16] and experimentally,[17–20] since its first observation[21] in NH_2. It might appear that the Renner-Teller (RT) effect in a tetra-atomic molecule should be a simple extension of that in a tri-atomic molecule, as in the model of Petelin and Kiselev.[22] However Pratt *et al.*[10] had observed seven members of the *trans*-bending progression of $C_2H_2^+$ ($v_4=0-3$, $K=0-2$) and had found that they did not fit well to this model. Later, Perić *et al.*[23–26] showed that the combination levels of ν_4 and ν_5 in $C_2H_2^+$ will be very complicated because of the different strengths of the vibronic coupling in the two bending vibrations. With the single exception of HCCS,[27–29] most of the RT effects in tetra-atomic molecules studied so far, such as $C_2H_2^+$,[10] HCCSe,[30] CaCCH,[31] and some Rydberg states of C_2H_2 and C_2D_2,[32–35] have been limited to one bending vibration because of the

[a]Also at Department of Chemistry, National Taiwan University, Taipei 10617, Taiwan, Republic of China.
[b]Also at Department of Applied Chemistry, National Chiao Tung University, Hsinchu, Taiwan 300, Republic of China.
[c]Also at Department of Chemistry, National Taiwan University, Taipei 10617, Taiwan, Republic of China. Electronic mail: ychsu@po.iams.sinica.edu.tw

constraints of Franck-Condon factors or the selection rules required by symmetry.

In this work, we have used a two-color ZEKE photoelectron spectroscopy technique, similar to that of Pratt *et al.*,[10] to observe the bending level structure of $C_2H_2^+$ up to 3520 cm^{-1}. Several different rotational and vibrational levels of the $\tilde{A}\ ^1A_u$ state of C_2H_2 were chosen as the intermediates for this two-color experiment. Comparison of the spectra from these different levels was very useful in clarifying the rotational assignments for some of the highly congested bands at higher energies. Altogether, 12 *trans*-bending levels (ν_4), 6 *cis*-bending levels (ν_5), and 23 combination levels, with K values up to 4, have been assigned in this work. In addition, we show that the relative signs of the Renner parameters in the two bending vibrations and the strength of the coupling between them are important in determining the detailed structure of the bending levels of $C_2H_2^+$.

II. EXPERIMENTAL DETAILS

Our ZEKE photoelectron spectrometer was designed and constructed following Müller-Dethlefs *et al.*'s pioneering design.[36,37] Briefly, it consists of a pulsed supersonic beam assembly, a pulsed-laser photoexcitation region, and a time-of-flight mass spectrometer. The skimmed molecular beam passes into the photoexcitation region, which is contained within a set of electrodes onto which a pulsed electric field is applied. The pulsed electric field, generated by a wave-form synthesizer (LeCroy 9112), is time-delayed with respect to each laser pulse to separate fast electrons spatially from slow electrons, to field-ionize high-n Rydberg molecules selectively and to accelerate electrons toward a 12-cm-long time-of-flight mass spectrometer. The photoexcitation region, at a distance of about 200 nozzle-diameters downstream from a skimmer, was kept at 10^{-7} torr, a nearly collision-free condition. The molecular beam consisted of a mixture of 20% acetylene in helium, expanded through a pulsed valve with a 500-μm nozzle diameter from a backing pressure of 1.5 atm.

The intermediate state in the double resonance, reached by the first laser, was a single rotational level of the $\tilde{A}\ ^1A_u$ state of C_2H_2 in one of the $4\nu_3$ ($K=1-2$), $5\nu_3$ ($K=1$), $\nu_2+4\nu_3$ ($K=0$) states, or the $K=1$ state at 47 206 cm^{-1}. (The state at 47 206 cm^{-1}, assigned by Van Craen *et al.*[38] as 1^13^2, was recently shown[39] to be a high bending level, though an updated vibrational assignment has not yet been offered.) The second laser frequency was scanned to obtain pulsed-field-induced (PFI) ZEKE photoelectron spectra up to 11.8 eV. The linewidth of the frequency-doubled output of our pulsed dye laser (Lambda-Physik, FL3002) is about 0.25 cm^{-1}.

Figure 1(a) shows the temporal profile of the delayed pulsed field used in this work. Two pulsed electric fields, each of strength ~0.1 V/cm but with opposite polarities, were applied at time delays of 200 and 1000 ns, respectively, after the optical excitation. These have the effect of field-ionizing Rydberg molecules with principal quantum numbers n near 300.[37,40] The first pulse, F_1, drives away those electrons resulting from direct photoionization, and its strength was chosen so as to be slightly stronger than the stray field,

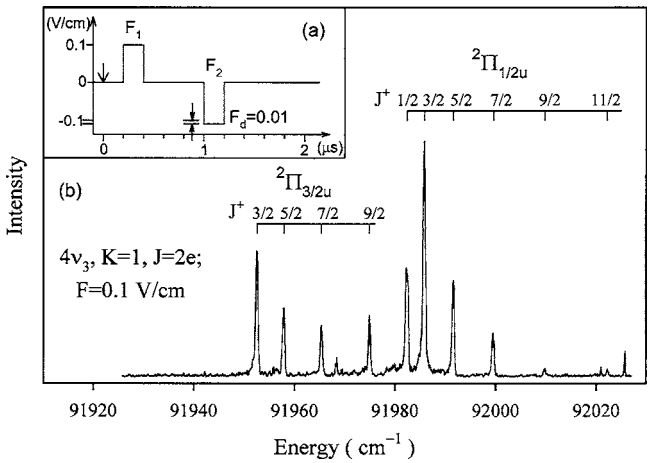

FIG. 1. (a) Time profile of the two pulsed electric fields which are applied to extract high-n Rydberg states. The spectral resolution of the PFI-ZEKE spectrum is determined by F_d, which is the absolute field strength of $|F_2-F_1|$. In this work, F_1, F_2, and F_d were chosen as 100, 110, and 10 mV/cm, respectively. (b) The PFI-ZEKE spectrum of the zero-point level of the acetylene cation obtained by using the e-parity component of the $\tilde{A}\ ^1A_u$, $4\nu_3$, $K=1$, $J=2$ level as the intermediate.

estimated to be about 50 mV/cm. The difference between the magnitudes of the two fields, $|F_2|-|F_1|$, was set to 0.01 V/cm; this determines which cluster of Rydberg levels is field ionized, and therefore governs the linewidth. The narrowest linewidth we could obtain in our PFI-ZEKE spectra was about 0.4–0.6 cm^{-1}, as illustrated in Fig. 1.

In this work, we have recorded PFI-ZEKE spectra at total energies in the range of 91 930–95 485 cm^{-1}. The energies of the states of the cation are the sums of the photon energies of the two lasers. The absolute energies of the rotational levels of the $\tilde{A}$ state reached by the first laser were taken from Van Craen *et al.*,[38] while the absolute frequency of the second laser was calibrated against optogalvanic lines from a Fe–Ne hollow cathode lamp. The calibration uncertainty in the individual measurements of the energies of the cation states is estimated to be no greater than 0.25 cm^{-1}, with the exceptions of the lowest Π_u levels from $4\nu_4$ and $6\nu_4$, where the uncertainties are up to 0.4 and 4 cm^{-1}, respectively. For the weaker transitions, it was sometimes necessary to average two or more spectra.

III. DESCRIPTION OF THE OBSERVED LEVELS AND THEIR ASSIGNMENT

A total of 43 vibrational bands has been recorded with rotational resolution in PFI-ZEKE spectra of C_2H_2 in the energy range of 91 930–95 485 cm^{-1}. All except two of these can be assigned to bending levels with $\upsilon_4=0-6$, $\upsilon_5=0-3$, and $K=0-4$.

A. Propensity rules for rotational and vibrational transitions

The intensities of rotational lines in the PFI-ZEKE spectra depend on many factors, such as the exact nature of the orbital from which the electron is ionized, and therefore cannot be easily predicted ahead of time. Instead the strongest rotational transitions can be described as following propen-

sity rules.[41–46] In the present instance, the propensity rules are found to be $\Delta N=0, \pm1, \pm2$ and $\Delta K=0, \pm1, \pm2$. Specifically, $\Delta K=0$ transitions are much stronger than $\Delta K\neq 0$ transitions, with the intensity ratio of $\Delta K=0$ to $\Delta K=\pm2$ transitions estimated to be 10:1; at the same time the ratio of $\Delta K=-1$ to $\Delta K=+1$ transitions is about 2:1. Unfortunately, we cannot estimate the relative intensities of $\Delta K=0$ and $\Delta K=\pm1$ transitions.

Acetylene in the intermediate $\tilde{A}\,^1A_u$ state of our experiments is *trans*-bent.[47–49] In accord with the Franck-Condon principle the strongest vibrational bands in the PFI-ZEKE spectrum should therefore form a progression in the ν_4^+ (trans-bending) vibration of the $\tilde{X}\,^2\Pi_u$ state of $C_2H_2^+$. This is also consistent with simple symmetry arguments. An electronic transition from the $\tilde{A}\,^1A_u$ state would reach a *gerade* upper state if ionization did not occur. However, when it does, the outgoing electron comes from an orbital corresponding to the π_g molecular orbital of the linear configuration. This orbital has roughly the same shape as an atomic *d* orbital so that, when the ionization occurs, the outgoing electron has to have *p* or *f* partial wave character according to the selection rule $\Delta\ell=\pm1$. Odd-ℓ angular momentum states are *ungerade*, so that to preserve the *gerade* overall symmetry one expects to see prominent transitions to the *ungerade* vibronic levels of the cation. Since the ν_4 vibration has species π_g, all its vibrational levels will have *ungerade* symmetry in the $\tilde{X}\,^2\Pi_u$ state of $C_2H_2^+$.

Weak transitions to the combination levels $n\nu_4^+ + m\nu_5^+$ and a very weak ν_5^+-progression are also observed in our spectra. This is somewhat surprising since transitions from the $\tilde{A}$ state of C_2H_2 to levels involving ν_5^+ in the $C_2H_2^+$, $\tilde{X}$ state are Franck-Condon forbidden and have never been observed previously.[10] Transitions to the Σ_g vibronic components of the ν_5^+ fundamental must be accompanied by outgoing electrons with even-ℓ partial wave character, indicating that the π_g orbital from which the electron is lost does not resemble an atomic *d* orbital all that closely.

B. The zero-point level, $(\nu_4^+, \nu_5^+)=(0,0)$

Two intermediate states, $\tilde{A}\,^1A_u$, $4\nu_3$, $K=1$ and 2, have been used to obtain ZEKE spectra of the zero-point vibrational level of the cation. Figure 1(b) shows a rotationally resolved $1+1'$ PFI-ZEKE spectrum of this level, where the $^2\Pi_{3/2}$ spin-orbit component is seen to lie below the $^2\Pi_{1/2}$, as expected for a π^3 electron configuration. The strongest rotational lines have ΔN in the range of +2 to −2, though weaker lines with larger values of $|\Delta N|$ were also observed. By fitting ten observed rotational levels with J^+ up to 11/2 in the two spin-orbit components, we determined the rotational and spin-orbit constants of this level to be 1.1031 ± 0.0007 and -30.83 ± 0.02 cm^{-1}, respectively; these results are in good agreement with values previously reported by Jagod *et al.*[6] No Λ doubling was observable at our resolution.

The ionization potential (IP) of acetylene has been reported by various groups,[8–10,50–52] with the published values ranging from 91 915±24 cm^{-1} to 91 996±40 cm^{-1}. The most recent measurement, from Ref. 10, is 91 952±2 cm^{-1} (see Note added to proof). The IP is the energy difference between the lowest rotational levels of $C_2H_2^+$ ($\tilde{X}^2\Pi_u$) and C_2H_2 ($\tilde{X}\,^1\Sigma_g^+$), but this cannot be measured directly in PFI-ZEKE experiments because of the effects of field ionization. We have recorded the ZEKE spectra of the zero-point level a number of times, with different values of the electric field ranging from 0.1 to 2 V/cm. Figure 2 shows the photon energies required to ionize the three lowest rotational levels, plotted against the square root of the electric field strength, *F*, applied at the photoexcitation zone. It is clear from the figure that the photon energy, *E*, is given accurately by the relation

$$E = E_0 + CF^{1/2}, \tag{1}$$

where the intercept E_0 is the true ionization energy for field-free conditions. Table I gives the E_0 values and the *C* coefficients for several rotational levels near the IP. The ionization potential of acetylene is determined to be 91 953.77±0.09 cm^{-1} (3σ). Table I also shows that the coefficient *C* is independent of *J*.

Except for the data shown in Fig. 2, all the spectra reported in this paper were recorded at a field strength of

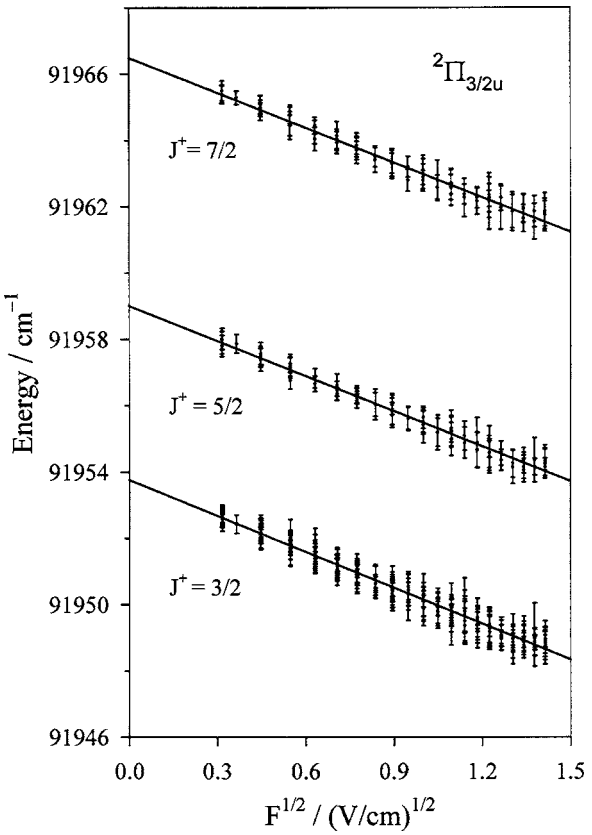

FIG. 2. Observed ionization energies of the first three rotational levels of the $\tilde{X}\,^2\Pi_{3/2,u}$, $\upsilon=0$ state of $C_2H_2^+$, plotted as a function of the square root of the extraction field. Several determinations were made for each level at each value of the field strength, *F*; the results are shown as dots, with the line widths [full width at half maximum (FWHM)] indicated by vertical bars. Extrapolation to zero field gives the "true" ionization energy for each rotational level. The ionization potential of C_2H_2, from the lowest rotational level of the neutral molecule to the lowest rotational level of the cation, is 91 953.77±0.03 cm^{-1}.

TABLE I. Ionization energies from the C_2H_2, $\tilde{X}\,^1\Sigma_g^+$, $v=0$, $J=0$ level to the lowest rotational levels of the zero-point vibrational level of $C_2H_2^+$, $\tilde{X}\,^2\Pi_u$.

Spin-orbit component	J^+	E_0/cm^{-1}	$C/(V/cm)^{1/2}$
$^2\Pi_{3/2,u}$	3/2	91 953.77±0.03	−3.61±0.03
	5/2	91 959.00±0.05	−3.51±0.05
	7/2	91 966.51±0.05	−3.53±0.05
	9/2	91 976.25±0.05	−3.52±0.04
	11/2	91 988.03±0.05	−3.44±0.06
	13/2	92 002.00±0.05	−3.54±0.05
$^2\Pi_{1/2,u}$	1/2	91 983.57±0.04	−3.51±0.05
	3/2	91 986.98±0.04	−3.50±0.04
	5/2	91 992.74±0.04	−3.47±0.04
	7/2	92 000.76±0.04	−3.52±0.04
	9/2	92 011.00±0.04	−3.42±0.04
	11/2	92 023.45±0.09	−3.49±0.11

100 mV/cm. Since $C \approx -3.5\ cm^{-1}/(V/cm)^{1/2}$, an energy correction of about 1.1 cm^{-1} must be added to all the level energies given elsewhere in this paper.

The values of the coefficient C are consistent with values previously reported,[40] indicating that the molecules undergo a diabatic ionization process,[40,53–55] where the rate of change of the pulsed electric field is fast compared to the adiabatic passage of the Rydberg molecule through the pattern of avoided crossings in the Stark manifold.

C. The two bending fundamentals, $v_4^+=1$ and $v_5^+=1$

Six vibronic bands have been observed at energies between 480 and 900 cm^{-1} above the (0,0) band. Their upper states are the components of the two bending fundamentals, ν_4 and ν_5. For both vibrations two Σ vibronic components and a Δ component are expected. Two strong bands at total energies of 92 453 and 92 863 cm^{-1} (vibrational energies of 487 and 897 cm^{-1}, respectively) could be immediately assigned to the Σ_u vibronic components of ν_4; their $1+1'$ PFI-ZEKE spectra, obtained via various different intermediate rotational levels ($\tilde{A}$, $4\nu_3$, $K=1$, $J=1-8$), are displayed in Fig. 3. The evidence for the Σ upper state symmetry is that the final rotational levels, as reached from a given intermediate level, have N^+ values that are either only even or only odd; if the upper states were degenerate, every N^+ value would have been present. The Kronig symmetries of the states (Σ^+ or Σ^-) can be deduced with the help of Fig. 4, which shows the possible transitions allowed by the conservation of nuclear spin symmetry and total parity. For the 92 453 cm^{-1} state the nuclear spin statistics are consistent only with $^2\Sigma_u^-$ or $^2\Sigma_g^+$ symmetry; the Franck-Condon and orbital considerations (as just described) then show that it must be a $^2\Sigma_u^-$ state. Similar arguments show that the 92 863 cm^{-1} state is $^2\Sigma_u^+$. These two bands had been assigned previously by Pratt *et al.*;[10] the vibronic energies found here agree with their values to within ±6 cm^{-1}. Pratt *et al.*[10] also deduced that the vibronic coupling parameter ε_4 is positive (because the $^2\Sigma_u^-$ state lies below the $^2\Sigma_u^+$ state) and that the outgoing

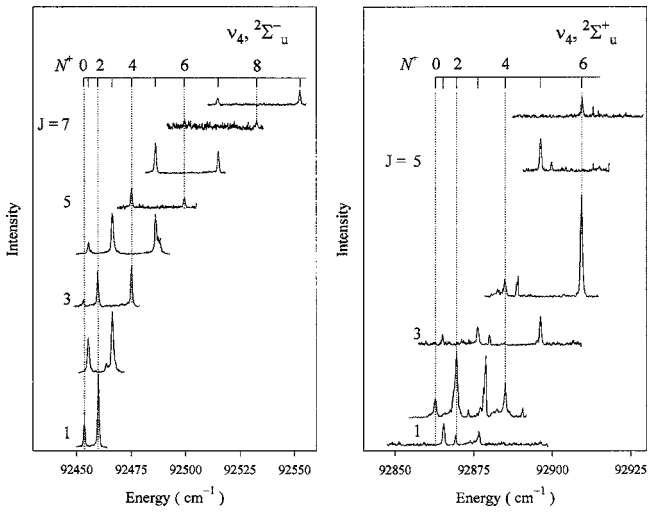

FIG. 3. PFI-ZEKE spectra of the two Σ components of the ν_4 fundamental of $C_2H_2^+$. The left-hand panel shows the rotational structure of its lower Renner component, $^2\Sigma_u^-$, where eight traces were recorded from eight intermediate levels, $\tilde{A}\,^1A_u$, $3\nu_4$, $K=1$, $J=1-8$. The right-hand panel shows its upper Renner component, $^2\Sigma_u^+$; six spectra were obtained from $J=1-6$ of the same intermediate vibrational state.

electrons involved in these transitions must carry odd partial waves, since the optical transition requires a change of the overall parity.

The strongest lines in these two bands follow $\Delta N=0$ and ±1; higher values, such as $\Delta N=\pm 2$ and ±3, were sometimes found in weaker lines. In making the line assignments it was necessary to compare the spectra taken via several different intermediate-J levels in order to establish which N^+ levels were in common. In this way, we could distinguish the spurious sharp lines from the slightly broader PFI-ZEKE spec-

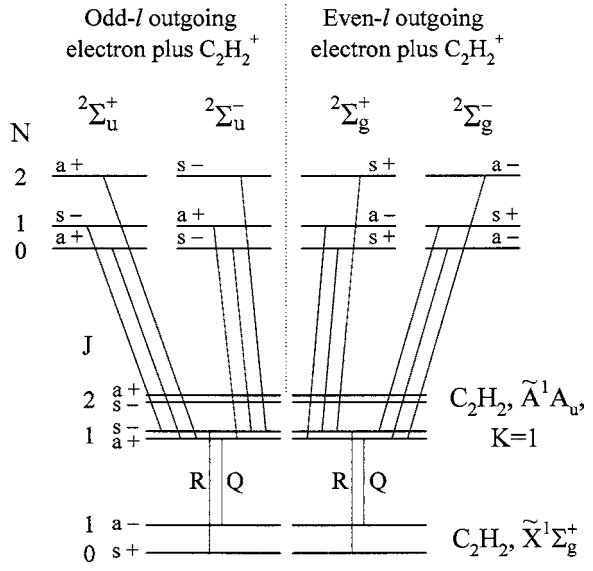

FIG. 4. Double resonance transitions from the ground state of acetylene, via an $\tilde{A}\,^1A_u$, $K=1$ state, to the four types of $^2\Sigma$ vibronic states belonging to the $^2\Pi_u$ ground state of the cation. The outgoing electrons carry odd-ℓ partial waves when *ungerade* states of the ion result, and even-ℓ partial waves when *gerade* states of the ion result. The nuclear spin state is conserved in the ionization process (a=antisymmetric, s=symmetric with respect to exchange of the two proton spins). The + and − signs indicate the total parity. The spin-rotation doubling of the $^2\Sigma$ states is not shown.

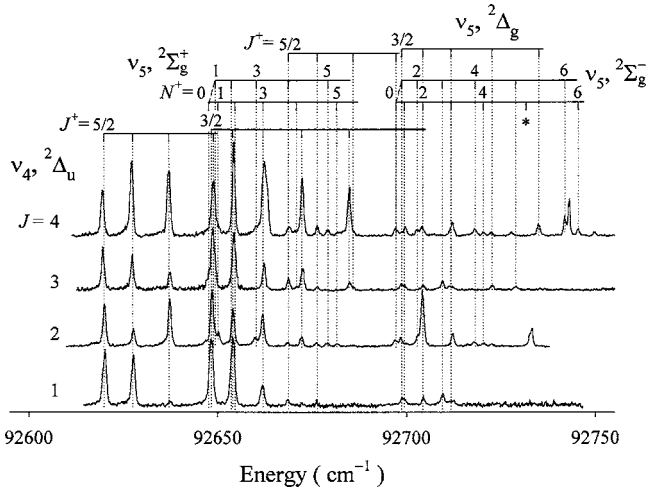

FIG. 5. 1+1′ PFI-ZEKE spectra of the acetylene cation in the region of the bending fundamentals near 92 675 cm^{-1}. Two Δ states and two Σ states can be identified. The strong band at the low-frequency side is assigned to the Δ_u component of the ν_4 (*trans*-bending) fundamental; the other weaker lines are the three components of the ν_5 (*cis*-bending) fundamental. The negative sign of ε_5 is established by the energy order of the $^2\Sigma_g^-$ and $^2\Sigma_g^+$ components of the ν_5 fundamental. The F_1 component of the $^2\Sigma_g^+$, $N=5$ level is not observed; its calculated position is marked with an asterisk.

tral lines. Other authors[56] have also reported that strong sharp lines from auto-ionization processes often mask nearby PFI-ZEKE lines.

The splitting between these two $^2\Sigma_u$ levels determines the quantity $\varepsilon_4\omega_4$ as 205 cm^{-1}; this is much larger than the spin-orbit coupling parameter $A_{so}=-31.5$ cm^{-1}, so that the electron spin effects are almost entirely quenched in them. In essence, the vibration-orbit coupling (Renner-Teller effect) is so much stronger than the spin-orbit coupling that the latter is reduced to a minor detail. According to Eqs. (27) and (28) of Ref. 13, the spin-orbit coupling in these Σ components becomes an apparent spin-rotation interaction, whose size is governed by the ratio $A_{so}/\varepsilon\omega$. For the ν_4 vibration these equations predict that the apparent spin-rotation parameters, γ, in the two levels should be about 0.006 cm^{-1}. This is far too small to be observed at our resolution.

In between the two Σ bands just described, near 92 675 cm^{-1}, are another strong band and three very weak bands; they are illustrated in Fig. 5. The strong band can be assigned as the $^2\Delta_u$ component of the ν_4 fundamental on the following grounds: it has two spin components, with roughly the same separation as in the zero-point level, the first J^+ levels are $J^+=2.5$ and 1.5, and both parities are present for each J^+ value. The ν_4 assignment follows from Franck-Condon arguments. These observations agree with those of Pratt *et al.*[10] The weak lines centered near 92 695 cm^{-1} have been assigned to the three components of the ν_5 fundamental; they were not reported in Ref. 10 and are observed here for the first time. To bring up the signal-to-noise ratio for these very weak bands, it was necessary to co-add several scans taken under the same conditions. Even so, some of the weak lines are not easy to pick out. Examples are the lowest N^+ lines of the lower Σ vibronic band, which are mostly obscured by strong transitions to the $^2\Delta_{3/2u}$ component of ν_4. It can be seen in Fig. 5 how the Σ vibronic bands show only even- or only odd-N^+ lines depending on the J value of the intermediate state, just as in Fig. 3. Using arguments based on Fig. 4 again, the lower energy Σ vibronic level is assigned as $^2\Sigma_g^+$ and the upper as $^2\Sigma_g^-$. The relative order of these Σ states immediately determines the sign of ε_5 as negative, while the fact that they are separated by only 19 cm^{-1} more than the spin-orbit splitting of the $\tilde{X}\,^2\Pi_u$ state shows that ε_5 is very small. The remaining lines in this region are assigned as transitions to the Δ_g component of ν_5. It is clear that ν_4 and ν_5 have quite similar frequencies, because the mean position of the two ν_4, Σ_u levels is only 14 cm^{-1} below the mean of the two ν_5, Σ_g levels.

Consistent with the small size of $\varepsilon_5\omega_5$, the apparent spin-rotation splitting in the Σ components of the ν_5 fundamental is expected to be quite large. The formulae of Ref. 13 predict $\gamma=0.50$ and 0.46 cm^{-1}, respectively, for the upper and lower Σ_g states, giving splittings that should be easily resolvable at our resolution. As described above, the lowest-N levels are quite severely blended for both components, but clear spin-rotation splittings can be seen in Fig. 5 for the $N=5$ level of the $^2\Sigma_g^+$ state and the $N=4$ level of the $^2\Sigma_g^-$ state. The two spin components are seen to have equal intensities in both bands. Band-by-band fits have been carried out for these two states, giving spin-rotation constants $\gamma=0.56\pm0.04$ and 0.46 ± 0.05 cm^{-1}, respectively, for the upper and lower Σ_g components; these appear to be in satisfactory agreement with the formulae of Ref. 13. It is not possible to determine the signs of the γ parameters from the observed spectra, but they should always be positive according to Ref. 13.

Band-by-band fits have been carried out for all the various upper levels. Their assignments, term values, rotational and spin constants are listed in Table II. More details of these are given in Sec. V, below.

D. The $v_4^+ + v_5^+ = 2$ levels

The overtones $2\nu_4$ and $2\nu_5$ are each expected to consist of three vibronic states, two of species Π_u and one of species Φ_u. The combination level $\nu_4+\nu_5$ should have four components, of species Π_g, Π_g, Π_g, and Φ_g. We have identified nine of these ten components, which lie in the energy range of 93 000–93 600 cm^{-1}. The only unobserved state is the upper Π_u component of the $2\nu_4$ level.

The assignment of the components can be understood with the help of the correlation diagram given as Fig. 6. In the center of the figure is the complete structure, including the unobserved Π_u component, calculated from the results of the final least squares fit, described in Sec. V, below. On the left hand side are the two overtones, $2\nu_4$ and $2\nu_5$, and the three components into which they each split as a result of the vibration-orbit coupling. Only the anharmonicity and the effects of the vibronic coupling terms in $\varepsilon_4\omega_4$ and $\varepsilon_5\omega_5$ are included. As might be expected from the fundamentals, the splitting of the *trans*-bending overtone, $2\nu_4$, is much larger than that of the *cis*-bending overtone, $2\nu_5$. The central component of each overtone is of species Φ_u. These Φ_u levels are "unique" levels,[15] meaning that they do not interact with any other Φ_u levels with the same vibrational quantum numbers because none such exist. As a result they should lie at the

TABLE II. Results of band-by-band fits to the observed vibronic levels of the $\tilde{X}\,^2\Pi_u$ state of $C_2H_2^+$. Values in cm^{-1}. Where more than one component with the same symmetry occurs in a vibrational state, its place in order of increasing energy is given by labels 1–5. The values of T_{ev} have not been corrected for the downward shift of about 1.1 cm^{-1} caused by the 100 mV/cm electric field used in this work. The numbers in parentheses following the parameter values are one standard deviation in units of the last significant figure quoted. σ=root-mean-square (rms) deviation of the fit. The intermediate levels in the double resonance have been coded as follows: $4^1=4\nu_3$, $K=1$; $4^2=4\nu_3$, $K=2$; $5^1=5\nu_3$, $K=1$; U=unassigned $K=1$ level at 47 206 cm^{-1}; $2^0=\nu_2+4\nu_3$, $K=0$. J_{max} is the largest value of J assigned for the state.

	E_{vib}	T_{ev}	B	A_{so}	γ	σ	Intermediate	J_{max}	Notes
$v=0(\Pi_u)$	0.000	91 965.859(12)	1.10311(67)	−30.827(16)	⋯	0.02	$4^1,4^2$	5.5	
$\nu_4(\Sigma_u^-)$	487.302	92 453.161(25)	1.10303(55)	⋯	⋯	0.07	$4^1,4^2$	9.5	
$\nu_4(\Delta_u)$	665.668	92 631.527(95)	1.1021 (25)	−29.37(12)	⋯	0.19	$4^1,4^2$	8.5	
$\nu_5(\Sigma_g^+)$	682.08	92 647.94 (19)	1.0875 (93)	⋯	0.464 (46)	0.19	$4^1,4^2$	5.5	
$\nu_5(\Delta_g)$	715.13	92 680.99 (18)	1.0978 (91)	−30.82(23)	⋯	0.24	$4^1,4^2$	5.5	
$\nu_5(\Sigma_g^-)$	731.209	92 697.068(87)	1.1168 (56)	⋯	0.561 (39)	0.16	$4^1,4^2$	6.5	
$\nu_4(\Sigma_u^+)$	897.167	92 863.026(69)	1.1047 (31)	⋯	⋯	0.15	4^1	6.5	
$2\nu_4(\Pi_u)-1$	1095.182	93 061.041(89)	1.1171 (43)	−2.42(20)	⋯	0.16	$4^1,4^2$	6.5	
$\nu_4+\nu_5(\Pi_g)-1$	1195.431	93 161.290(27)	1.1132 (17)	0	⋯	0.05	$4^1,4^2$	5.5	
$2\nu_4(\Phi_u)$	1325.231	93 291.090(72)	1.1063 (42)	−27.232(83)	⋯	0.08	$4^1,4^2$	6.5	
$\nu_4+\nu_5(\Pi_g)-2$	1360.699	93 326.558(74)	1.1103 (38)	−29.115(95)	⋯	0.13	$4^1,4^2$	5.5	
$2\nu_5(\Pi_u)-1$	1379.47	93 345.33 (16)	1.125 (12)	−2.85(49)	0.280 (98)	0.13	$4^1,4^2$	4.5	
$\nu_4+\nu_5(\Phi_g)$	1383.70	93 349.56 (15)	1.0941 (54)	−30.09(22)	⋯	0.22	$4^1,4^2$	7.5	
$2\nu_5(\Phi_u)$	1432.356	93 398.215(54)	1.0904 (28)	−30.108(63)	0	0.04	$4^1,4^2$	6.5	[a]
$2\nu_5(\Pi_u)-2$	1443.600	93 409.459(97)	1.1243 (69)	0	0.378 (33)	0.12	$4^1,4^2$	4.5	
$\nu_4+\nu_5(\Pi_g)-3$	1601.354	93 567.213(43)	1.1258 (26)	0	⋯	0.07	5^1	5.5	
$3\nu_4(\Sigma_u^-)$	1672.909	93 638.768(33)	1.1123 (20)	⋯	⋯	0.06	$U,4^2,5^1$	5.5	
$3\nu_4(\Delta_u)-1$	1732.759	93 698.618(38)	1.1052 (17)	−5.054(58)	⋯	0.06	$U,4^2,5^1$	6.5	
$2\nu_4+\nu_5(\Sigma_g^+)-1$	1790.323	93 756.182(52)	1.1063 (32)	⋯	⋯	0.10	$U,4^2,5^1$	5.5	
$2\nu_4+\nu_5(\Sigma_g^-)-1$	1803.165	93 769.024(98)	1.1270 (86)	⋯	⋯	0.16	$U,4^2,5^1$	4.5	
$2\nu_4+\nu_5(\Delta_g)-1$	1808.66	93 774.52 (16)	1.1133 (84)	−2.45(29)	⋯	0.21	$U,4^2$	5.5	[b]
$\nu_4+2\nu_5(\Sigma_u^-)-1$	1891.444	93 857.303(39)	1.1076 (35)	⋯	⋯	0.07	U	4.5	
$\nu_4+2\nu_5(\Delta_u)-1$	1907.547	93 873.406(61)	1.1171 (28)	0	⋯	0.10	U	6.5	
$2\nu_4+\nu_5(\Delta_g)-2$	2012.52	93 978.38 (13)	1.0668 (71)	−26.54(19)	⋯	0.18	U	6.5	
$\nu_4+2\nu_5(\Sigma_u^+)-1$	2043.80	94 009.66 (10)	1.0700 (75)	⋯	1.265 (42)	0.17	U	4.5	
$\nu_4+2\nu_5(\Delta_u)-2$	2067.08	94 032.94 (16)	1.1148 (84)	−30.29(25)	⋯	0.20	U	6.5	[c]
$\nu_4+2\nu_5(\Sigma_u^-)-2$	2075.524	94 041.383(86)	1.1435 (81)	⋯	1.432 (50)	0.14	U	4.5	
$\nu_4+2\nu_5(\Gamma_u)$	2103.55	94 069.41 (35)	1.132 (21)	−23.3(24)	−1.59(49)	0.17	U	7.5	[d]
$4\nu_4(\Pi_u)-1$	2288.212	94 254.071(28)	1.1063 (25)	−2.971(85)	0.052 (19)	0.03	$2^0,4^2$	4.5	
$3\nu_4+\nu_5(\Pi_g)-1$	2376.717	94 342.576(95)	1.123 (14)	0	⋯	0.11	$U,5^1$	3.5	
$4\nu_4(\Phi_u)-1$	2387.12	94 352.98 (13)	1.1065 (42)	−7.80(19)	⋯	0.20	4^2	8.5	
$3\nu_4+\nu_5(\Pi_g)-2$	2424.98	94 390.84 (25)	1.098 (35)	−4.62(35)	⋯	0.25	5^1	3.5	
$2\nu_4+2\nu_5(\Pi_u)-1$	2489.39	94 455.25 (18)	1.1168 (52)	0	⋯	0.40	$U,5^1$	8.5	
$2\nu_4+2\nu_5(\Pi_u)-2$	2507.57	94 473.43 (19)	1.1129 (65)	⋯	⋯	0.41	$U,5^1$	7.5	
$2\nu_4+2\nu_5(\Phi_u)-1$	2524.15	94 490.01 (79)	1.080 (98)	−2.72(91)	⋯	0.39	$U,5^1$	4.5	
$\nu_4+3\nu_5(\Pi_g)-1$	2589.712	94 555.571(42)	1.1272 (61)	0	⋯	0.05	5^1	3.5	
$5\nu_4(\Sigma_u^-)$	2885.849	94 851.708(29)	1.0957 (17)	⋯	⋯	0.05	5^1	5.5	
$5\nu_4(\Delta_u)-1$	2930.643	94 896.502(36)	1.1089 (16)	−6.275(52)		0.05	5^1	6.5	
$2\nu_4+2\nu_5(\Pi_u)-5$	3079.86	95 045.72 (11)	1.1331 (65)	0	⋯	0.19	$U,5^1$	5.5	
$3\nu_4+\nu_5(\Pi_g)-4$	3185.02	95 150.88 (14)	1.1317 (62)	0	⋯	0.27	U	6.5	
$6\nu_4(\Pi_u)-1$	3519.359	95 485.218(73)	1.1151 (64)	−5.86(11)	⋯	0.10	2^0	4.5	[e]
$\nu_2+\nu_4(\Delta_u)$	2495.45	94 461.31 (15)	1.0805 (57)	−25.68(20)	0	0.24	5^1	7.5	[f]
?	2990.900	94 956.759(67)	1.1108 (26)	−6.45(10)	⋯	0.11	5^1	6.5	[g]

[a]Only five lines were included in the fit. A lower rms error, 0.007 cm^{-1}, is found if γ is floated, but the resulting value, $\gamma=-0.238$ (40) cm^{-1} seems unreasonable for a unique Φ state.
[b]Two lines ($J=3.5$ and 4.5) in the $P=3/2$ component were excluded from the fit.
[c]Only two lines ($J=1.5$ and 3.5) in the $P=3/2$ component were included in the fit.
[d]Only two lines ($J=3.5$ and 4.5) in the $P=7/2$ component were observed and included in the fit; the large value of γ may therefore be an artifact.
[e]Calibration uncertain.
[f]Only one $P=3/2$ line could be found. If γ is floated the resulting parameters (see text) are $T_{ev}=94\,461.60(12)$, $B=1.0736(37)$, $A=-27.21(43)$ cm^{-1}, $\gamma=0.48(14)$ cm^{-1}, with a rms error of 0.13 cm^{-1}. An alternative numbering of the $P=3/2$ line gives $A\approx-32$ cm^{-1}.
[g]Assignment uncertain, possibly $4\nu_4+\nu_5$, Δ_g.

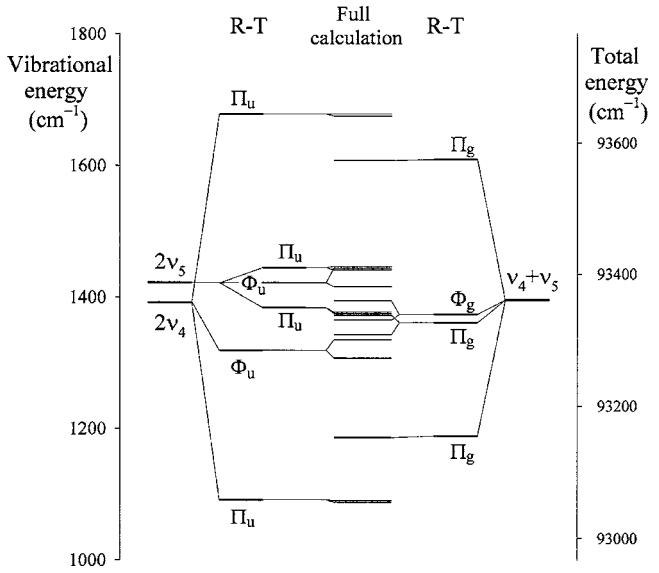

FIG. 6. The vibronic energy levels of $C_2H_2^+$, $\tilde{X}\,^2\Pi_u$ with $\upsilon_4+\upsilon_5=2$, calculated from the final constants from the least squares fit. The columns headed R-T show the splittings caused by the anharmonicity and the terms in $\varepsilon_4\omega_4$ and $\varepsilon_5\omega_5$; the central column shows the full level structure drawn to scale, including the g_K terms and the spin-orbit coupling.

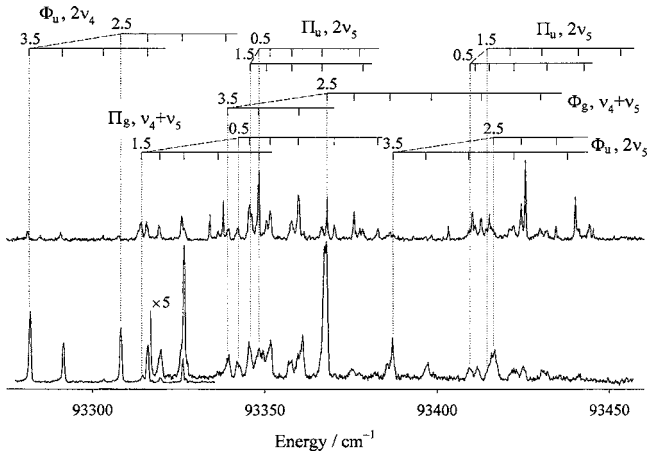

FIG. 7. $1+1'$ PFI-ZEKE spectra of $C_2H_2^+$ in the total energy range of 93 275–93 455 cm^{-1}, showing the six central components of the $\nu_4+\upsilon_5=2$ group of levels. The intermediate C_2H_2, $\tilde{A}\,^1A_u$ levels were: Upper trace, $4\nu_3$, $K=1$, $J=2$; Lower trace, $4\nu_3$, $K=2$, $J=2$. Diagonal tie lines connect the spin-orbit components of the states of the cation. The two $2\nu_5$, Π_u states are in Hund's case (b) coupling, with opposite signs for their spin-orbit splittings, whereas the $\nu_4+\nu_5$, Π_g state at 93 330 cm^{-1} is in case (a) coupling.

centers of their manifolds, in first approximation, and carry the full spin-orbit coupling of the electronic state. However, there are $\Delta\upsilon=2$ matrix elements of the vibronic coupling operator[11] that mix them with higher vibrational levels of the same K value, so that they are pushed down below the midpoints of the manifolds; the detailed matrix elements are given in Sec. IV, below. (This effect is not seen for $2\nu_5$ because the anharmonicity outweighs the very small off-diagonal vibronic coupling elements.) At the same time the mixing reduces the effective spin-orbit coupling parameter slightly. By contrast the Π_u levels occur in pairs, one of which lies considerably above the central Φ_u component, and one of which lies considerably below. In these nonunique levels the expectation value of the orbital angular momentum, $\langle L_z\rangle$, is almost zero; the spin-orbit coupling is therefore greatly reduced, so that Hund's spin-coupling case (b) is found. As explained by various authors,[13,57,58] the reason why $\langle L_z\rangle$ is so small in these levels is that their eigenfunctions contain nearly equal percentages of $|\Lambda=1\rangle$ and $|\Lambda=-1\rangle$ factors, which contribute oppositely to $\langle L_z\rangle$.

The right-hand side of Fig. 6 shows the splitting of the combination level $\nu_4+\nu_5$. Its structure can be understood as follows. The ν_4 fundamental of the $^2\Pi_u$ state consists of three widely spaced components, Σ^-, Δ, and Σ^+, as we have just seen. Since $\varepsilon_5\omega_5$ is small compared to $\varepsilon_4\omega_4$ we can ignore its effect on the energy levels in first approximation and, to form the combination levels, just add the vibrational angular momentum, $\ell_5=1$. The resulting components become Π, $\Pi+\Phi$, and Π, respectively. Now the Δ (central) component of the ν_4 fundamental is a unique level, so that the Π component derived from it must behave as a unique level, carrying the full spin-orbit coupling modified only by the higher order effects. The same will be true for the Φ component. None of the six other Π levels with $\upsilon_4+\upsilon_5=2$ behave this way, because in them the orbital angular momentum is reduced almost to zero.

Figure 7 shows the central portion of the PFI-ZEKE spectrum in this region, as recorded via the $\tilde{A}$, $4\nu_3$, $J=2e$, $K=1$ and 2 levels (upper and lower traces, respectively). Six bands are present, three with Φ upper states and three with Π upper states, as shown by the J numbering of their first levels. With $K=1$ as the intermediate, all the strong lines go to the Π states, with the Φ states barely visible. The opposite is found when $K=2$ is the intermediate; the Φ states carry nearly all the intensity. This is as expected from the propensity rules discussed earlier. The strongest of the three bands with Φ upper states, which lies near 93 300 cm^{-1}, could be assigned at once to the Φ_u component of the $2\nu_4$ level from Franck-Condon arguments. The assignments of the other two Φ states were based on preliminary values of ω_4, ω_5, ε_4, and ε_5 estimated from the bending fundamentals, just described.

As for the Π components, it can be seen that the Π state near 93 330 cm^{-1} has a large spin-orbit splitting, similar to that of the Φ states, but the other two, at 93 345 and 93 415 cm^{-1}, have almost no spin-orbit splitting. The Π state at 93 330 cm^{-1} is therefore the central Π_g component of the $\nu_4+\nu_5$ level.

It should be noted in Fig. 6 that the overall splitting of the $\nu_4+\nu_5$ level is smaller than that of the $2\nu_4$ overtone. The reason is that the overall splitting of a level υ varies[11] roughly as $\upsilon+1$. Since the splitting of ν_5 is small compared to that of ν_4, the overall splitting of $\nu_4+\nu_5$ will be similar to that of ν_4, while that of $2\nu_4$ will be about 1.5 times larger. Another consequence of the small splitting of ν_5 is that four of the Π levels of the $\upsilon_4+\upsilon_5=2$ group will be well separated from the rest, but there will be a cluster of six levels in the middle. This cluster corresponds to the region of the spectrum shown in Fig. 7.

The only level of this group reported in Ref. 10 is the lower $^2\Pi_u$ component of $2\nu_4$; our results are consistent with theirs.

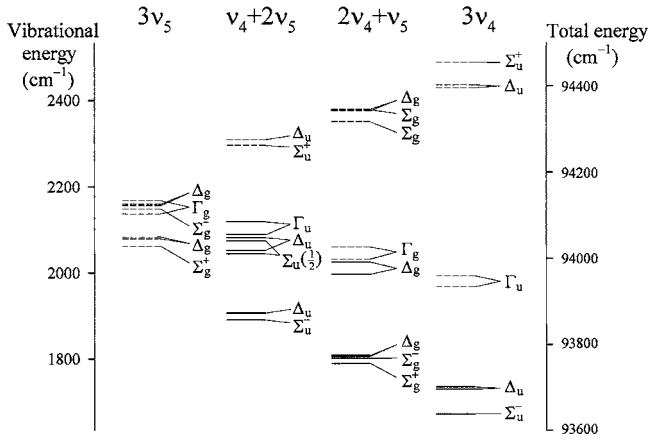

FIG. 8. The vibronic levels of $C_2H_2^+$, $\tilde{X}\,^2\Pi_u$, with $v_4^+ + v_5^+ = 3$. Levels drawn with solid lines were observed in this work; levels drawn with dashed lines are predicted from the results of the final least squares fit.

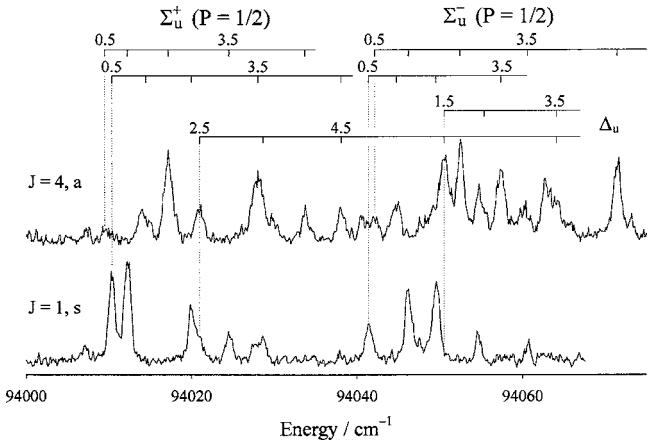

FIG. 9. $1+1'$ PFI-ZEKE spectrum of C_2H_2 near 94 040 cm^{-1}, showing part of the central group of vibronic states from the $\nu_4+2\nu_5$ vibrational level. The two Σ_u states show large spin-rotation splittings, indicating that they should be considered as $P=1/2$ states in case (a) coupling; their separation is seen to be almost the same as the spin-orbit splitting of the overlapping Δ_u state. The intermediate states were the $J=4$, a and 1, s rotational levels of the $\tilde{A}\,^1A_u$, $K=1$ state at 47 206 cm^{-1}.

E. The $v_4^+ + v_5^+ = 3$ levels

Twenty six vibronic levels are expected for $v_4^+ + v_5^+ = 3$; of these we have observed 12. These are the lower Σ and Δ levels of $3\nu_4$, two Σ levels and two Δ levels from $2\nu_4+\nu_5$ and six levels from $\nu_4+2\nu_5$, including two Δ levels and a Γ level. No vibronic levels of $3\nu_5$ were observed; this is to be expected since the Franck-Condon factors for transitions to the *cis*-bending levels are small. The assignments could mostly be made using calculations based on parameters from the lower vibrational levels, although some complications were met. Figure 8 is an energy level diagram of the complete vibronic level structure. Solid lines indicate the levels that were observed. Dashed lines represent the unobserved levels whose positions were calculated from the constants given by the final least squares fit, described in Sec. V.

The most interesting levels in this manifold are the Σ levels from $\nu_4+2\nu_5$. Their structures can be predicted using similar arguments to Sec. III D. The ν_4 fundamental in the $\tilde{X}\,^2\Pi_u$ state has Σ^-, Δ, and Σ^+ components, in order of increasing energy, where the Δ level is unique; the $2\nu_5$ overtone has $\ell = 0^+(\Sigma^+)$ and $2(\Delta)$ vibrational angular momentum states. Ignoring the effects of $\varepsilon_5\omega_5$, since they are very small, and adding the angular momenta, the $\nu_4+2\nu_5$ combination level will have components $\Sigma^-+\Delta$, $\Sigma^+ + \Sigma^- + \Delta + \Gamma$ (unique), and $\Sigma^+ + \Delta$. The levels will form three groups, reflecting the splitting of the ν_4 fundamental. The structure of the central group requires some discussion. The levels are derived from the Δ component of the ν_4 fundamental which, being unique, carries the full spin-orbit coupling of the $^2\Pi_u$ state. Although this is not very big in absolute terms, it is larger than the vibration-orbit (Renner-Teller) coupling in ν_5. This is analogous to the limiting case where $A_{\text{spin-orbit}} \gg \varepsilon\omega$ in a triatomic molecule, discussed by Hougen.[13] In that situation the pair of Σ^+ and Σ^- levels from the bending fundamental in a $^2\Pi$ state turns into two $P=1/2$ states separated by $A_{\text{spin-orbit}}$. We therefore expect that the central group of levels from $\nu_4+2\nu_5$ in $C_2H_2^+$ will consist of a Δ level and a Γ level, in Hund's case (a) coupling, plus two $P=1/2$ levels separated by the spin-orbit interval. All these levels are, in fact, seen. Figure 9 illustrates the PFI-ZEKE spectra of the two $P=1/2$ levels, recorded using intermediate states with odd and even J values. There is some overlapping by other bands, but the structure is clear, particularly in the lower tracing. The rotational lines show large splittings, which give rise to the obvious pairs. In a case (b) description the splittings are the spin-rotation doublings of the rotational levels, indexed by N. However, the splittings are almost as large as the separations of successive rotational levels, so that it is more meaningful to describe them in case (a) terms, where the pattern-forming quantum number is J rather than N. The splittings are then the parity doublings of the rotational levels, indexed by J. The assignments are given this way in Fig. 9.

The transformation of these two $P=1/2$ states to case (a) coupling is not complete, so that it is still possible to determine their Kronig symmetries using the nuclear spin statistics. With the help of Fig. 4 it is seen that the lower state is Σ_u^+ and the upper state is Σ_u^-. This is opposite to what is found in the ν_4 fundamental.

We have also observed the $^2\Sigma_u^-$ level from the lowest group of $\nu_4+2\nu_5$ levels. Since it is not derived from a unique level it follows Hund's case (b) coupling, with a very small spin-rotation parameter. Assuming that these combination levels can be treated as if they were pure ν_4 levels, the calculated value of γ, using the equations in Ref. 13, is about 0.006 cm^{-1}; this is again far too small for us to observe. To our knowledge this is the first instance where Σ states belonging to the same vibrational level have been found to have different spin couplings.

In this energy region Pratt *et al.*[10] reported just two bands, which they assigned to the $^2\Sigma_u^-$ and lower $^2\Delta_u$ components of $3\nu_4$. Our data for these levels are consistent with theirs.

F. The $v_4^+ + v_5^+ \geqslant 4$ levels

Ten of the 35 levels with $v_4^+ + v_5^+ = 4$ appear in our spectra: they are illustrated in the energy level diagram of Fig. 10. As expected from Franck-Condon arguments, the observed lev-

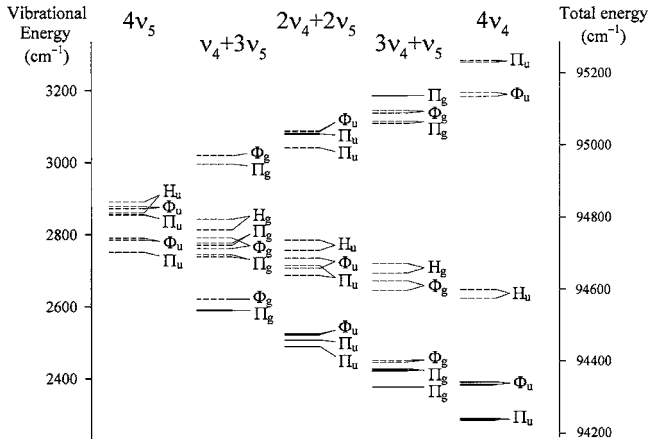

FIG. 10. Energy level diagram of the vibronic levels of $C_2H_2^+$, $\tilde{X}\,^2\Pi_u$, with $v_4^+ + v_5^+ = 4$. Levels drawn with solid lines were observed in this work, levels drawn with dashed lines were calculated from the spectroscopic parameters in Table III.

els have predominantly *trans*-bending character and, with a single exception, can be assigned to the vibrational levels $4\nu_4$, $3\nu_4+\nu_5$, and $2\nu_4+2\nu_5$. Nearly all of the observed levels belong to the lower Renner-Teller components though, somewhat surprisingly, two upper Renner-Teller components have been identified; these are the highest Π levels belonging to $3\nu_4+\nu_5$ and $2\nu_4+2\nu_5$. Figure 11 illustrates the two lowest components of $4\nu_4$, near 94 300 cm^{-1}; these have species $^2\Pi_u$ and $^2\Phi_u$. The lowest $^2\Pi_g$ component of $3\nu_4+\nu_5$ occurs at almost the same energy as the $^2\Phi_u$ state, but could be distinguished from it by judicious choice of the intermediate state in the double resonance: if the $\tilde{A}\,^1A_u$, $4\nu_3$, $K=2$ level is chosen as the intermediate, the $^2\Pi_g$ level is completely suppressed.

The only assigned states with higher vibrational quantum numbers belong to the pure *trans*-bending levels $5\nu_4$ and $6\nu_4$, again as expected from the Franck-Condon principle. The lowest vibronic components of $5\nu_4$ and $6\nu_4$ are illustrated in Fig. 12. Lying just below the $6\nu_4$, $^2\Pi_u$ band is some further structure to which we have not been able to assign vibrational quantum numbers, though it is clear that a $K=0$ and a $K=1$ level are present. At this energy combination levels involving ν_1 or ν_2 with the bending vibrations could be contributing to the observed structure.

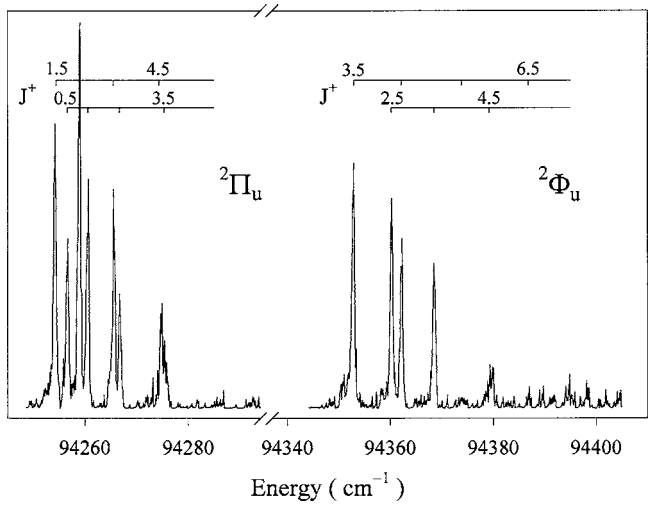

FIG. 11. 1+1′ PFI-ZEKE spectra of $C_2H_2^+$ in the energy range of 94 250–94 400 cm^{-1}, showing the lowest two components of the $4\nu_4$ level of the cation. The intermediate states for the $^2\Pi_u$ and $^2\Phi_u$ components were the $J=2$ rotational levels of the $\tilde{A}\,^1A_u$, $\nu_2+4\nu_3$, $K=0$ and $4\nu_3$, $K=2$ states, respectively.

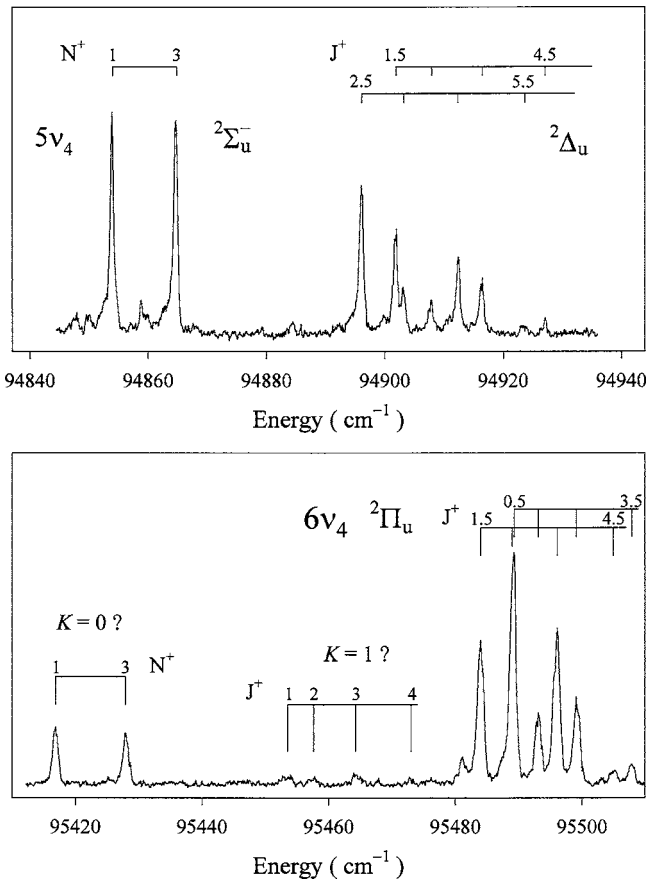

FIG. 12. 1+1′ PFI-ZEKE spectra of the acetylene cation, $\tilde{X}\,^2\Pi_u$. Upper trace: the lowest $^2\Sigma_u^-$ and $^2\Delta_u$ components of the $5\nu_4$ overtone; the intermediate state was the $J=2e$ level of the $\tilde{A}\,^1A_u$, $5\nu_3$, $K=1$ state. Lower trace: the lowest $^2\Pi_u$ component of the $6\nu_4$ overtone, together with unidentified $K=0$ and 1 states; the intermediate was the $J=2$ level of $\tilde{A}\,^1A_u$, $\nu_2+4\nu_3$, $K=0$.

G. Further unassigned levels

Near 94 460 cm^{-1} we found what appears to be a Δ level among the low energy components of the $v_4^+ + v_5^+ = 4$ group where no Δ level is predicted. The lines of the lower spin component, $^2\Delta_{5/2}$, are fairly strong and easy to number, but the upper spin component is weaker and so badly overlapped by the two lowest Π_u components of $2\nu_4+2\nu_5$ that only one line lies in the clear. The most likely vibrational assignment is to the Δ_u component of $\nu_2+\nu_4$, since its vibrational energy of 2495 cm^{-1} is close to the sum of ν_2 (1829 cm^{-1} according to Ref. 8) and the Δ component of ν_4 (665.7 cm^{-1}). The most reasonable numbering for the one clear line leads to T_{ev} = 94 461.31(15) cm^{-1}, B = 1.0805(57) cm^{-1}, and A_{so} = −25.68(20) cm^{-1}, with an rms error of 0.24 cm^{-1}; a rather lower rms error (0.13 cm^{-1}) is found if γ is floated, but the resulting value, γ=0.48(14) cm^{-1} seems very unlikely for a unique Δ level. Alternative J numberings for the clear line

TABLE III. Vibrational and electronic parameters from global least-squares fits to the rotational levels with $v_4+v_5\leqslant 2$ and 5 in the $\tilde{X}\,^2\Pi_u$ ground electronic state of $C_2H_2^+$. Values in cm^{-1}. Numbers in parentheses are one standard deviation in units of the last significant figure quoted.

	$v_4+v_5\leqslant 2$	$v_4+v_5\leqslant 5$
T_0[a]	90 577.38 (46)	90 578.30 (45)
B	1.1028 (11)	1.1045 (15)
A_{so}	−31.283(66)	−31.535(84)
ω_4	688.92 (29)	689.01 (26)
ω_5	719.39 (35)	718.29 (44)
$\varepsilon_4\omega_4$[b]	204.923 (82)	205.62 (10)
$\varepsilon_5\omega_5$	−19.690(45)	−20.094(72)
ε_{554}	−3.920(60)	−4.408(80)
g_{K4}	1.720 (31)	1.810 (32)
g_{K5}	4.545 (47)	4.721 (44)
g_{44}	1.322 (54)	0.778 (17)
g_{45}	7.039 (73)	6.330 (47)
g_{55}	3.625 (82)	3.543 (27)
x_{44}	2.634 (56)	2.674 (66)
x_{55}	−2.684(66)	−2.53(11)
x_{45}	−4.316(90)	−4.51(18)
r_{45}		−2.661(39)
y_{444}		0.0481 (61)
y_{455}		0.148 (47)
α_5		0.0091 (17)
No. of levels[c]	164	364
rms	0.210	0.340

[a]T_0 is an effective parameter, which does not include the zero-point energies for ν_4 and ν_5, and has not been corrected for the downward shift of about 1.1 cm^{-1} caused by the 100 mV/cm electric field used in this work.
[b]Derived coupling parameters: $\varepsilon_4=0.2974_6$, $\varepsilon_5=-0.0273_7$.
[c]Number of rotational levels included in the fit.

lead to improbable values for the spin-orbit constant. As for ν_2 itself, Pratt *et al.*[10] found some weak features between 93 755 and 93 780 cm^{-1} which they assigned tentatively to this vibration, but these do not appear in our spectra.

A complicated band group near 95 050 cm^{-1} appears to contain a Δ_g level from $4\nu_4+\nu_5$, a Δ_u level from $3\nu_4+2\nu_5$ and the highest Π_u level from $2\nu_4+2\nu_5$; it is weak and severely overlapped, so that the assignments are not certain. These levels were not included in the final least squares fits. All the vibronic levels for which the assignments are secure are listed in Table II.

IV. THEORY

Table III gives the results of global least squares fits to the assigned rotational levels, in which the parameters for the vibronic and spin-orbit coupling are determined. This section gives the underlying theory, after which a discussion of the least squares results follows.

The $^2\Pi_u$ ground electronic state of $C_2H_2^+$, which arises from the configuration $\ldots(\pi_u)^3$, has electronic angular momentum $|\Lambda|=1$ and unpaired electron spin, $S=1/2$. Besides the usual vibration-rotation terms the Hamiltonian must therefore include the vibration-orbit coupling (Renner-Teller effect) and the spin-orbit interaction. The effective Hamiltonian we have used is given as Eqs. (2)–(6),

$$H = H_{\text{vib}} + H_{\text{rot}} + H_{\text{RT}} + H_{\text{spin-orbit}}, \tag{2}$$

where

$$\begin{aligned} H_{\text{vib}} = {} & T_0 + \omega_4(v_4+1) + \omega_5(v_5+1) + x_{44}(v_4+1)^2 \\ & + x_{55}(v_5+1)^2 + y_{444}(v_4+1)^3 \\ & + y_{445}(v_4+1)(v_5+1)^2 \\ & + g_{44}\ell_4^2 + g_{55}\ell_5^2 + g_{45}\ell_4\ell_5 + x_{45}(q_{4+}q_{4-}q_{5+}q_{5-}) \\ & + (1/4)r_{45}(q_{4+}^2q_{5-}^2 + q_{4-}^2q_{5+}^2), \end{aligned} \tag{3}$$

$$H_{\text{rot}} = B[(J^2 - J_z^2) - (J_+S_- + J_-S_+)], \tag{4}$$

$$\begin{aligned} H_{\text{RT}} = {} & (1/2)\varepsilon_4\omega_4(q_{4+}^2e^{-2i\theta} + q_{4-}^2e^{+2i\theta}) \\ & + (1/2)\varepsilon_5\omega_5(q_{5+}^2e^{-2i\theta} + q_{5-}^2e^{+2i\theta}) \\ & + (1/2)\varepsilon_{554}q_5^2(q_{4+}^2e^{-2i\theta} + q_{4-}^2e^{+2i\theta}) + g_{K4}G_{4z}L_z \\ & + g_{K5}G_{5z}L_z, \end{aligned} \tag{5}$$

$$H_{\text{spin-orbit}} = A_{so}L_zS_z. \tag{6}$$

In these equations the symbols q, J, L, S, and G represent dimensionless operators for the vibrational normal coordinates, the total angular momentum, the electron orbital angular momentum, the electron spin angular momentum, and the vibrational angular momentum, respectively. The angle θ is the azimuth angle of the unpaired electron relative to an arbitrary reference plane containing the linear molecule. The other quantities are parameters or quantum numbers.

In this work, we consider only those vibrational levels where the two bending modes ν_4 and ν_5 are excited, because no effects such as Fermi or Coriolis resonances have been observed. Since both ν_4 and ν_5 are doubly degenerate vibrations, two quantum numbers, v and ℓ, are needed to index each of their vibrational levels. The quantum number ℓ represents the vibrational angular momentum. The operators for the vibrational normal coordinates, $q_{n\pm}=q_{nx}\pm iq_{ny}$, $n=4$ and 5, act to change both v and ℓ either upwards or downwards by one unit.

The vibronic terms in Eq. (5) consist of Renner's operators for the coupling of electronic and vibrational motion[11] and the g_K parameters introduced by Brown *et al.*[16,59,60] to account for the mixing of excited Σ and Δ electronic states into the Π state. We have also added a coupling cross term (in ε_{554}) which was found to be necessary for the combination levels; its form follows from an extension of Brown's work. For simplicity we have taken the parameter ε_{554} to have the dimensions of cm^{-1}, unlike ε_4 and ε_5 which are dimensionless. According to Gauyacq and Jungen,[61] the quartic anharmonic corrections to the energies of the levels will probably be of the same order of magnitude as the g_K parameters, and should be considered together with them. In $C_2H_2^+$ there will be two terms representing the difference between the quartic force constants for the Born-Oppenheimer components of the $^2\Pi_u$ state, one for ν_4 and one for ν_5. These have the same form as the ε_{554} term of Eq. (5) except that all the subscripts are the same, that is

$$H_{\text{quartic}} = (1/2)\varepsilon_{444}q_4^2(q_{4+}^2 e^{-2i\theta} + q_{4-}^2 e^{+2i\theta}) + (1/2)\varepsilon_{555}q_5^2(q_{5+}^2 e^{-2i\theta} + q_{5-}^2 e^{+2i\theta}). \quad (7)$$

We experimented with adding these terms to the Hamiltonian, but ε_{555} turned out to be essentially zero, while ε_{444} was very small (about 0.04 cm^{-1}) and barely determined ($\leqslant 2.5\sigma$). They were not included in the final least squares fits. The ε_{iii} parameters of Eq. (7) correspond to the g'_{22} parameter of Ref. 61.

To our knowledge this study is the most comprehensive that has been carried out so far for the bending levels of a symmetrical tetra-atomic molecule in an electronic Π state. We therefore give a detailed list of the matrix elements used, although many of them are taken from previous authors.[11,16,62–64] The rotational basis functions for calculation of the matrix elements have been taken as the simple products $|\Lambda;v_4,\ell_4,v_5,\ell_5;K\rangle|S,\Sigma\rangle|J,P\rangle$, where P is the projection of J along the axis of the linear molecule, $P=\Lambda+\ell_4+\ell_5+\Sigma=K+\Sigma$. The phase factors for these basis functions follow from the relation

$$\sigma_v|\Lambda;v_4,\ell_4,v_5,\ell_5;K\rangle|S,\Sigma\rangle|J,P\rangle = (-1)^{\Lambda}(-1)^{S-\Sigma}(-1)^{J-P}|-\Lambda;v_4,-\ell_4,v_5,-\ell_5;-K\rangle |S,-\Sigma\rangle|J,-P\rangle. \quad (8)$$

In this basis the vibrational terms in Eq. (3) are all diagonal except for the last two, which have complicated matrix elements because the vibrations ν_4 and ν_5 are degenerate. The diagonal element of the x_{45} term is just[62]

$$\langle v_4,\ell_4,v_5,\ell_5|H_{\text{vib}}|v_4,\ell_4,v_5,\ell_5\rangle = x_{45}(v_4+1)(v_5+1), \quad (9)$$

but the off-diagonal elements are

$$\langle v_4\pm 2,\ell_4,v_5\pm 2,\ell_5|H_{\text{vib}}|v_4,\ell_4,v_5,\ell_5\rangle = (1/4)x_{45}[(v_4+\ell_4+1\pm 1)(v_4-\ell_4+1\pm 1)\times(v_5+\ell_5+1\pm 1)(v_5-\ell_5+1\pm 1)]^{1/2},$$

$$\langle v_m,\ell_m,v_n\pm 2,\ell_n|H_{\text{vib}}|v_m,\ell_m,v_n,\ell_n\rangle = (1/2)x_{45}(v_m+1)[(v_n+\ell_n+1\pm 1)\times(v_n-\ell_n+1\pm 1)]^{1/2}, \quad (10)$$

$$\langle v_m-2,\ell_m,v_n+2,\ell_n|H_{\text{vib}}|v_m,\ell_m,v_n,\ell_n\rangle = (1/4)x_{45}[(v_m+\ell_m)(v_m-\ell_m)\times(v_n+\ell_n+2)(v_n-\ell_n+2)]^{1/2},$$

where m and n are 4 or 5.

The term in r_{45} is responsible for various vibrational ℓ-type resonance effects[62–64] which include the separation of the Σ^+ and Σ^- components of the combination level $\nu_4+\nu_5$ in a nondegenerate electronic state. Its matrix elements are

$$\langle v_m,\ell_m+2,v_n,\ell_n-2|H_{\text{vib}}|v_m,\ell_m,v_n,\ell_n\rangle = (1/4)r_{45}[(v_m-\ell_m)(v_m+\ell_m+2)(v_n+\ell_n)\times(v_n-\ell_n+2)]^{1/2},$$

$$\langle v_m,\ell_m+2,v_n\pm 2,\ell_n-2|H_{\text{vib}}|v_m,\ell_m,v_n,\ell_n\rangle = (1/8)r_{45}[(v_m-\ell_m)(v_m+\ell_m+2)(v_n\mp\ell_n+1\pm 1)\times(v_n\mp\ell_n+1\pm 3)]^{1/2},$$

$$\langle v_m\pm 2,\ell_m+2,v_n,\ell_n-2|H_{\text{vib}}|v_m,\ell_m,v_n,\ell_n\rangle = (1/8)r_{45}[(v_m\pm\ell_m+1\pm 1)(v_m\pm\ell_m+1\pm 3)(v_n+\ell_n)\times(v_n-\ell_n+2)]^{1/2}, \quad (11)$$

$$\langle v_m\pm 2,\ell_m+2,v_n+2,\ell_n-2|H_{\text{vib}}|v_m,\ell_m,v_n,\ell_n\rangle = (1/16)r_{45}[(v_m\pm\ell_m+1\pm 1)(v_m\pm\ell_m+1\pm 3)\times(v_n-\ell_n+2)(v_n-\ell_n+4)]^{1/2},$$

$$\langle v_m\pm 2,\ell_m+2,v_n-2,\ell_n-2|H_{\text{vib}}|v_m,\ell_m,v_n,\ell_n\rangle = (1/16)r_{45}[(v_m\pm\ell_m+1\pm 1)(v_m\pm\ell_m+1\pm 3)\times(v_n+\ell_n)(v_n+\ell_n-2)]^{1/2}.$$

Again m and n are 4 or 5. The Darling-Dennison resonance[63,64] between the overtones of ν_4 and ν_5 comes from the third formula of Eq. (10) and the last two formulas of Eq. (11).

The matrix elements of the vibronic terms in Eq. (5) are diagonal in K. The g_K terms are diagonal in all quantum numbers,[16]

$$\langle\Lambda;v_4,\ell_4,v_5,\ell_5;K|H_{\text{RT}}|\Lambda;v_4,\ell_4,v_5,\ell_5;K\rangle = g_{K4}\ell_4\Lambda + g_{K5}\ell_5\Lambda, \quad (12)$$

but the elements of the terms in $\varepsilon\omega$ are off-diagonal in Λ,[11]

$$\langle\Lambda=-1;v\pm 2,\ell+2|H_{\text{RT}}|\Lambda=1;v,\ell\rangle = -(\varepsilon\omega/4)[(v\pm\ell+1\pm 1)(v\pm\ell+1\pm 3)]^{1/2}$$

$$\langle\Lambda=-1;v,\ell+2|H_{\text{RT}}|\Lambda=1;v,\ell\rangle = -(\varepsilon\omega/2)[(v-\ell)(v+\ell+2)]^{1/2}. \quad (13)$$

Equation (13) applies to both ν_4 and ν_5, with appropriate subscripts added. The term in ε_{554} has elements with the same quantum number dependence as Eq. (13), which are obtained by writing $\varepsilon_4\omega_4+\varepsilon_{554}(v_5+1)$ for $\varepsilon_4\omega_4$ throughout in that equation; it also has further elements,

$$\langle\Lambda=-1;v_4,\ell_4+2,v_5\pm 2,\ell_5|H_{\text{RT}}|\Lambda=1;v_4,\ell_4,v_5,\ell_5\rangle = -(\varepsilon_{554}/4)[(v_4-\ell_4)(v_4+\ell_4+2)(v_5+\ell_5+1\pm 1)\times(v_5-\ell_5+1\pm 1)]^{1/2},$$

$$\langle\Lambda=-1;v_4+2,\ell_4+2,v_5\pm 2,\ell_5|H_{\text{RT}}|\Lambda=1;v_4,\ell_4,v_5,\ell_5\rangle = -(\varepsilon_{554}/8)[(v_4+\ell_4+2)(v_4+\ell_4+4)(v_5+\ell_5+1\pm 1)\times(v_5-\ell_5+1\pm 1)]^{1/2}, \quad (14)$$

$$\langle\Lambda=-1;v_4-2,\ell_4+2,v_5\pm 2,\ell_5|H_{\text{RT}}|\Lambda=1;v_4,\ell_4,v_5,\ell_5\rangle = -(\varepsilon_{554}/8)[(v_4-\ell_4)(v_4-\ell_4-2)(v_5+\ell_5+1\pm 1)\times(v_5-\ell_5+1\pm 1)]^{1/2}.$$

The various matrix elements from Eqs. (10)–(14) that are

off-diagonal in the vibrational quantum numbers give rise to matrices of infinite order. For the results given in Table III we truncated the matrices to be diagonalized at six quanta of both ν_4 and ν_5 beyond the highest level in the data set. Some preliminary calculations had been carried out with the truncation limit set to four quanta, but since the changes in the parameters on going to six quanta were within their error limits, we saw no point in going to yet larger matrices.

Only two terms were needed for the rotation and spin. The diagonal element is

$$\langle \Lambda; v_4, \ell_4, v_5, \ell_5; S, \Sigma; J | H_{\text{rot}} + H_{\text{spin-orbit}} | \Lambda; v_4, \ell_4, v_5, \ell_5; S, \Sigma; J \rangle = A_{\text{so}} \Lambda\Sigma + B[J(J+1) - P^2 - \langle S_\perp^2 \rangle] \quad (15)$$

and the off-diagonal (spin-uncoupling) element is

$$\langle \Lambda; v_4, \ell_4, v_5, \ell_5, K; S, \Sigma; J | H_{\text{rot}} | \Lambda; v_4, \ell_4, v_5, \ell_5, K; S, -\Sigma; J \rangle = -B[J(J+1) - (K-1/2)(K+1/2)]^{1/2}. \quad (16)$$

In Eq. (15) the quantity $\langle S_\perp^2 \rangle = \langle S_x^2 + S_y^2 \rangle$ has been taken as $S(S+1) - \langle S_z^2 \rangle = 1/2$ for a doublet state. For the band-by-band fits given in Table II a spin-rotation term, $(\gamma/2)$ $(J_+ S_- + J_- S_+)$, was added to the rotational Hamiltonian; its matrix elements are as Eq. (16) but with B replaced by $-\gamma/2$. This accounts for what remains of the spin-orbit coupling in the non-unique[15] levels, where the orbital angular momentum is coupled more strongly to the vibration.[13] The true spin-rotation interaction must be very small because, when the vibration-orbit coupling is taken into account by the matrix treatment of Eqs. (9)–(16), as for Table III, there is no need for a spin-rotation term.

The rotational constant B was treated as a separate parameter for each vibronic level in the band-by-band fits of Table II, but for the final fits given in Table III it was assumed to vary according to the simple expression $B_v = B + \Sigma_{i=4,5} \alpha_i v_i$. In fact only α_5 was determinable, and then only for the fit to the complete data set (second column of Table III).

V. RESULTS OF THE LEAST SQUARES FITTINGS

We have observed 41 vibronic levels with $\nu_4 \leqslant 6$, $\nu_5 \leqslant 3$, and $K \leqslant 4$ in the energy region 0–3500 cm^{-1} above the zero-point energy level of $C_2H_2^+$. Table II gives the rotational constants for these levels, as obtained from band-by-band fits to the rotational structure; specifically, it lists the band origins (T_{ev}), the effective B-values and spin constants, A_{so} or γ, the rms errors and the intermediate states used to record the spectra. A number of global fits were also carried out, in order to get the vibrational, spin, and the Renner-Teller parameters; the results from these are given in Table III. The assigned rotational line frequencies and the residuals given by the full global least squares fit are listed in the Supplementary material.[65]

A. Global least squares fit for levels with $v_4^+ + v_5^+ \leqslant 2$

The highest observed bending vibronic level of $C_2H_2^+$ with $v_4^+ + v_5^+ \leqslant 2$ lies more than 200 cm^{-1} below the lowest stretching level, the ν_2 (C≡C) fundamental at 1829 cm^{-1};[8] these low-lying bending levels are therefore not affected by any stretch-bend interactions, so that the parameters determined from them will give the clearest representation of the pure bending potentials. We have observed 16 of the 17 vibronic levels with $v_4 + v_5 \leqslant 2$, missing only the upper Π_u component of the $2\nu_4$ overtone. For the least squares fit we varied five vibronic parameters ($\varepsilon_4\omega_4$, $\varepsilon_5\omega_5$, ε_{554}, g_{K4}, and g_{K5}), nine vibrational parameters (T_0, ω_4, ω_5, x_{44}, x_{55}, x_{45}, g_{44}, g_{55}, and g_{45}), the spin-orbit constant A_{so}, and a single rotational constant B; the rms error was 0.21 cm^{-1}. No Darling-Dennison resonance parameter was included. The first column of Table III shows the parameters obtained and their standard deviations.

The internal consistency of the fit is demonstrated by the fact that all the spin effects, such as the variation of the spin-orbit coupling in the unique levels with v, could be treated with just one spin-orbit parameter. For instance, from Table II, the spin-orbit coupling of the Δ_g component of the ν_5 fundamental (in a band-by-band model) is seen to be almost exactly the same as that of the zero-point level, while that of the Δ_u component of the ν_4 fundamental is 1.46 cm^{-1} lower. Hougen[13] has shown that higher order vibronic effects cause the effective spin-orbit coupling constant in these unique levels to decrease with v (or K) according to

$$A_{\text{spin-orbit}}^{\text{unique}}(K = v+1) = A_0[1 - \varepsilon^2 K(K+1)/8]. \quad (17)$$

From the values in Table III the lowering of the effective spin-orbit constants for the $\nu_4(\Delta_u)$ and $\nu_5(\Delta_g)$ levels, compared to the zero-point level, should be 1.37 and 0.01 cm^{-1}; these quantities are very close to what is seen in Table II. Nevertheless, small systematic residuals in the spin-orbit structure of some of the Φ unique levels indicate that the derived value of A_{so} is slightly too small.

An interesting feature of the results is the large size of the g_K parameters that allow for the contamination of the $^2\Pi$ state by nearby $^2\Sigma$ and $^2\Delta$ states, as a result of vibronic coupling. Shifts resulting from these g_K parameters are responsible for some of the blending that complicates the assignments. For example the $^2\Delta_{3/2,g}$ spin-orbit component of the ν_5 fundamental is raised by just enough to be almost degenerate with the $^2\Sigma_g^-$ component (Fig. 5), and a similar effect occurs in the cluster at the center of the $v_4 + v_5 = 2$ group (Fig. 7). Not enough is known about the properties of the excited electronic states of $C_2H_2^+$ to identify which of them may be responsible for the g_K parameters.

B. Least squares fits including the levels with $\nu_4 + \nu_5 = 3-5 (\nu_5 \leqslant 3)$

The second column of Table III gives the results of a least squares fit to the observed rotational levels with $v_4 + v_5 \leqslant 5$. The parameters used were the same as those for the fit to the levels with $v_4 + v_5 \leqslant 2$, but with the addition of the vibration-rotation parameter α_5 and the anharmonicity parameters r_{45}, y_{444}, and y_{455}. All the assigned bending levels were included in the data set except the uppermost Π_u component of $2\nu_4 + 2\nu_5$ and the lower Π_u component of $6\nu_4$. The $2\nu_4 + 2\nu_5$, Π_u band is part of a complicated group of over-

lapped structure near 95 000 cm^{-1}. It gave residuals of about 4 cm^{-1}, which were not significantly reduced on adding higher order terms to the Hamiltonian such as the quartic terms in Eq. (7); it may be that combination levels involving ν_2 are interacting with the pure bending levels up at this comparatively high vibrational energy. The $6\nu_4$ level was omitted because its calibration is uncertain. The rms error was 0.34 cm^{-1}, which is somewhat larger than for the smaller data set, but the values of the principal parameters (other than g_{44}) change very little.

The results show that the various anharmonicity parameters for $C_2H_2^+$ are close to their values in the ground state of C_2H_2.[66] On the other hand the large size of α_5, which is quite well determined, but four times bigger than in the ground state of C_2H_2,[66] is surprising. The parameter which requires some discussion is the spin-orbit coupling. The value from the $v_4+v_5\leqslant 5$ data set is about 0.25 cm^{-1} higher than that from the $v_4+v_5\leqslant 2$ data set. This gives a slightly better fit to the low vibrational levels, almost eliminating the systematic residuals, but it overestimates the spin-orbit splittings of some of the higher levels. In particular, the calculated splittings of the Δ_g component of $2\nu_4+\nu_5$ and the Δ_u component of $\nu_4+2\nu_5$ are about 1 cm^{-1} too large. We attempted to correct these in the least squares fits by allowing A_{so} to vary with v_4 and v_5, but the results were inconclusive. It is clear that the effective value of A_{so} becomes smaller on excitation of ν_5 in these higher combination levels, but not in any simple way that is consistent with the lower levels involving ν_5.

The F_1 spin component of the $\nu_4+2\nu_5$, Σ_u^+ state was also omitted from the data set. This state is one of the case (a) Σ_u states that was discussed in Sec. III E, and illustrated in Fig. 9. It appears that the reason for the poor fit is the spin-orbit coupling again. If these Σ_u states are considered to be isolated $P=1/2$ states, the large splitting of their rotational levels can be described[13] by a P-doubling parameter, p,

$$\Delta\nu = p(J+1/2). \tag{18}$$

The smaller p is, the closer the vibronic state is to pure case (a) coupling. The observed value is $p\sim 0.87$ cm^{-1}, but the value obtained by fitting the final calculated line positions to Eq. (18) is about 0.51 cm^{-1}, meaning that the states are not as close to case (a) as the calculations would suggest. According to Ref. 13, pure case (a) occurs when the spin-orbit coupling totally dominates the vibronic coupling, which implies that the spin-orbit coupling in these Σ_u levels is smaller than the least squares results would predict. This is what was found also in the nearby Δ levels. As discussed above, we have not been able to find a satisfactory model for the apparently irregular variation of the spin-orbit coupling with vibration in these levels.

VI. DISCUSSION

In this work we have identified levels involving the ν_5 (*cis*-bending) vibration of the $\tilde{X}\,^2\Pi_u$ state of $C_2H_2^+$ for the first time, and determined the vibronic coupling parameter ε_5 as -0.0273_7. *Ab initio* calculations[23–26,67] have predicted the experimental ν_5 frequency of 719 cm^{-1} fairly closely, but there has been controversy over the sign and magnitude of ε_5, presumably because it is quite small. For example, the most recent calculations by Perić *et al.*[24] gave the frequency as 724 cm^{-1}, but the separation of the Σ_g^+ and Σ_g^- components of the ν_5 fundamental was given as 9 cm^{-1}, compared to the experimental value of 50 cm^{-1}.

This work is the most detailed account so far of the bending levels of a symmetrical tetra-atomic linear molecule in a degenerate electronic state. Because the lowest stretching frequency of $C_2H_2^+$ lies considerably above the manifold of $v_4+v_5=2$ levels, the structure is singularly free from Fermi resonance effects. It therefore provides excellent data for refining the theory of the Renner-Teller effect in such systems. It turns out that the bending fundamentals are well described by a simple extension of the theory for triatomic systems, and the lowest levels for which new higher order terms are required are the overtones $2\nu_4$ and $2\nu_5$. We have found that the interactions between the two vibrations can be modeled successfully with a term of the type ε_{554}, which essentially gives a v_5-dependence to the Renner parameter ε_4. Only this one term is needed, presumably because the vibronic coupling in ν_5 is very small, so that the variation in ε_5 with v_4 is negligible. Since $C_2H_2^+$ has a center of symmetry there is no cross term in the vibronic Hamiltonian with coefficient $\varepsilon_{45}(\omega_4\omega_5)^{1/2}$, such as Tang and Saito[27] had to introduce for the $\tilde{X}\,^2\Pi$ state of HCCS. A term of this type allows for interaction between the Σ components of the ν_4 and ν_5 fundamentals, but in $C_2H_2^+$ these levels have different u-g symmetry.

The ground state of HCCS provides the best data set for an unsymmetrical tetra-atomic molecule in a degenerate electronic state,[29] and a brief comparison with $C_2H_2^+$ is in order. The main difference is that Fermi resonance effects are very important for both HCCS and DCCS, because the ν_3 fundamental lies between the overtones $2\nu_4$ and $2\nu_5$; no fewer than four Fermi resonance parameters were needed to describe the levels of HCCS up to about 2000 cm^{-1}. It is interesting that the quantity $\varepsilon_4\omega_4$ is almost identical in the ground states of $C_2H_2^+$ and HCCS, because it implies that the ν_4 vibration in HCCS (the HCC bending mode) is very similar in character to the *trans*-bending vibration of $C_2H_2^+$. In both molecules ε_4 is much larger than ε_5, and of opposite sign. There was no need for a term in ε_{554} in HCCS, possibly because the strong Fermi resonances mask the need for such a term.

Interesting new effects occur in the combination levels of $C_2H_2^+$ as a result of the interplay of the two vibration-orbit couplings. For example, two different spin coupling cases are found for K-components of the same vibrational level. This cannot happen in overtones, but requires the excitation of two different bending vibrations where one of the ε parameters is large and the other is small. Perhaps the most unusual case occurs in the $\nu_4+2\nu_5$ vibrational level, where the two central Σ components are in case (a) coupling, separated by the spin-orbit interval, but the outer two are in case (b) coupling. This is a result of the small size of ε_5, which means that the effects of the vibronic coupling in ν_5 on the energy levels are negligible. The central Σ components are derived from the "unique" central component of the ν_4 fundamental,

which carries almost the full spin-orbit coupling of the electronic state. Essentially the spin still "sees" the orbital angular momentum even though it is disguised by the vibration. This situation will in fact occur for all K values, in the appropriate combination levels; for example, the central Π component of $\nu_4+\nu_5$ is in case (a) coupling while the outer Π components are close to case (b).

In the ν_4 fundamental the Σ_u^- component lies below the Σ_u^+ component, reflecting the positive sign of ε_4. The same is true for the outer Σ components of the $\nu_4+2\nu_5$ combination level but, interestingly, the energy order is reversed for its two central Σ components, where the Σ_u^+ component lies below the Σ_u^- (see Figs. 8 and 9). On closer examination it appears that this should always be so, because there are matrix elements of the vibronic coupling term in $\varepsilon_5\omega_5$ which act between the central and outer Σ states of the same symmetry. Omitting spin effects, the central Σ^+ and Σ^- components would be almost degenerate if ε_5 was vanishingly small, being separated only by the effects of the ℓ-type resonance term in r_{45} [Eq. (11)], but the vibronic coupling pushes each of the central Σ components away from its corresponding outer component, to give the reversed energy order. In the present case the spin-orbit coupling outweighs the effects of $\varepsilon_5\omega_5$, so that the two central states are better described as $P=1/2$ states; however, their Kronig symmetries can still be determined, and are found to be opposite to those of the outer components.

It is instructive to compare the energies of the states we have observed with the previous photoelectron results and with the analyses of the Rydberg transitions of C_2H_2. In their He 584 Å photoelectron spectra of the $\tilde{X}\,^2\Pi_u$ state Reutt *et al.*[8] assigned a vibrational peak at 1670 cm^{-1} to the $2\nu_4$ overtone. Interestingly, this corresponds to the one component of the $\nu_4+\nu_5=2$ polyad that we do not see, namely the predicted upper $^2\Pi_u$ component of $2\nu_4$ at 1676 cm^{-1}. They also reported[8] a "Renner-Teller multiplet" involving ν_5, but gave no further details. Estimating the band positions from their published spectra, we find that the two lower bands of the multiplet match to within 10 cm^{-1} with the Σ_g^+ component of ν_5 and the Σ_u^+ component of ν_4, but there is no match with their third feature near 1020 cm^{-1}. Its assignment remains an open question. On the other hand the previous PFI-ZEKE spectra of Pratt *et al.*[10] agree closely with our results, not surprisingly, since the technique and the choice of intermediate electronic state are essentially the same.

The $s\sigma$ and $d\sigma$ Rydberg states (of $^1\Pi_u$ symmetry) should show the Renner-Teller splittings that reflect the vibronic coupling of the ion core fairly accurately. Unfortunately predissociation complicates the assignment of most of the absorption bands, but fairly clear ν_4 sequence structure in the $4s\sigma\ \tilde{G}\,^1\Pi_u-\tilde{X}$ transition gives[32] rough values of $\omega_4=473$ cm^{-1} and $|\varepsilon_4|=0.39$. The frequency is somewhat lower than our ion core value of 689 cm^{-1}, but the separation of the Σ_u^+ and Σ_u^- components of the fundamental is only 40 cm^{-1} less than the ion core value. For the $3d\delta\,\tilde{H}\,^1\Pi_u$ state, Ref. 32 gives $\omega_4=550$ cm^{-1} and $|\varepsilon_4|=0.28$, which is closer to the ion core values. Their assignments of structure involving ν_5 may need to be revisited, since their value[32] of $|\varepsilon_5|=0.29$ seems out of line with the very small ion core value (Table III).

Colin *et al.*[32] analyzed the bending structure of the $\tilde{G}$ and $\tilde{H}$ states on the basis of a core-penetrating Rydberg electron, where the vibronic splittings are changed somewhat from those of the ion core. On the other hand Zhu *et al.*[68] found that the bending structure of the $3d\delta\,\tilde{F}'\,^1\Phi_u$ state was better described in terms of a non-penetrating electron, where the observed splittings are essentially those of the ion core, modified only slightly by the presence of the Rydberg electron. The structure they assigned for the ν_4 fundamental gives $\omega_4=768$ cm^{-1}, $\varepsilon_4=0.318$, values which are quite similar to those of Ref. 10. However, Fillion *et al.*[69] have found that some of the vibrational assignments of Ref. 68 are not confirmed by their deuterium isotope shift measurements.

Anderson and co-workers[1–3] have used 2+1 resonantly enhanced multiphoton ionization (REMPI), together with a quadrupole ion guide, to prepare $C_2H_2^+$ ions in various vibrational states, specifically the zero-point level, the C=C stretching fundamental (ν_2) or a bending overtone near 1270 cm^{-1}.[70] They found that, at low collision energies, the bending overtone excitation enhanced endothermic reactions, such as

$$C_2H_2^+ + CH_4 \rightarrow C_2H_3^+ + CH_3$$

and

$$C_2H_2^+ + OCS \rightarrow C_2H_2 + OCS^+,$$

more effectively than C=C stretching excitation.[1–3] Based on symmetry arguments and comparison with *ab initio* values they tentatively assigned the bending overtone as $2\nu_5$. However, our results do not support this assignment. The width of their bending overtone feature (~400 cm^{-1}) seems too large for the small vibration-orbit splitting of $2\nu_5$ while, as Fig. 6 shows, their reported frequency of ~1270 cm^{-1} is too low, and corresponds more closely to the Π_g component of $\nu_4+\nu_5$ or the Φ_u component of $2\nu_4$. Also the intermediate states they used have since been assigned[35] as ν_4 and ν_2 excitations in the $3p\,^1\Delta_g$ and $3p\,^1\Sigma_g^+$ states, so that on Franck-Condon grounds it is more likely that they were preparing *trans*-bending states of $C_2H_2^+$.

For the rotational constant B, our value of 1.1031_1 $(6_7,1\sigma)$ cm^{-1} from the band-by-band fit agrees favorably with the more accurate $B=1.104\,63(2)$ cm^{-1} from Ref. 6. Perhaps coincidentally, the value obtained from the full global least squares fit, 1.1045(15) cm^{-1}, agrees almost exactly with Ref. 6. The spin-orbit interval in the ground vibrational level was given indirectly as −30.91(2) cm^{-1} from the effects of spin uncoupling on the rotational structure of the ν_3 fundamental,[6] and has been measured directly as −30.70(1) cm^{-1} by Cha *et al.*[71] in their REMPI study of the $\tilde{A}-\tilde{X}$ system of $C_2H_2^+$; our value of −30.83(2) cm^{-1} is in satisfactory agreement.

Finally, we note that it might not have been possible to observe the $\nu_4+2\nu_5$ and $2\nu_4+\nu_5$ levels of $C_2H_2^+$ with such intensity without the fortunate choice of the $K=1$ level of the $\tilde{A}\,^1A_u$ state of C_2H_2 at 47 206 cm^{-1} as the intermediate state. Given its original assignment[38] as $\nu_1+2\nu_3$ one might have

expected to see mostly $n\nu_4$ levels of $C_2H_2^+$; the observation of strong bands involving ν_5 is consistent with its reassignment[39] to a level involving excitation of the *ungerade* bending modes of the $\tilde{A}\,^1A_u$ state.

Note added in proof. Since this paper was written, we have become aware of a more recent value for the ionization potential, $91\,953.5\pm0.5$ cm^{-1}, obtained by P. Rupper and F. Merkt [Rev. Sci. Instrum. **75**, 613 (2004)] using one-photon ZEKE spectroscopy.

ACKNOWLEDGMENTS

The authors thank the Academia Sinica and the National Science Council of Taiwan, R.O.C. (Grant Nos. NSC88-2113-M-001-025 and NSC89-2113-M-001-078) for financial support. One of the authors (Y.-C.C.) would like to acknowledge the Academia Sinica for a postdoctoral fellowship. The authors are also grateful to Dr. J. T. Hougen (NIST, Gaithersburg) and Professor A. J. Merer (UBC, Vancouver) for valuable assistance with parts of this work.

[1] T. M. Orlando, B. Yang, and S. L. Anderson, J. Chem. Phys. **92**, 7356 (1990).
[2] B. Yang, Y. Chiu, and S. L. Anderson, J. Chem. Phys. **94**, 6459 (1991).
[3] Y. Chiu, H. Fu, J. Hung, and S. L. Anderson, J. Chem. Phys. **101**, 5410 (1994); **102**, 1199 (1995).
[4] P. B. Armentrout and T. Baer, J. Phys. Chem. **100**, 12866 (1996), and references therein.
[5] P. Löffler, E. Wrede, L. Schnieder, J. B. Halpern, W. M. Jackson, and K. H. Welge, J. Chem. Phys. **109**, 5231 (1998).
[6] M.-F. Jagod, M. Roesslein, C. M. Gabrys, B. D. Rehfuss, F. Scappini, M. W. Crofton, and T. Oka, J. Chem. Phys. **97**, 7111 (1992).
[7] C. Baker and D. W. Turner, Chem. Commun. (London) **1967**, 797.
[8] J. E. Reutt, L. S. Wang, J. E. Pollard, D. J. Trevor, Y. T. Lee, and D. A. Shirley, J. Chem. Phys. **84**, 3022 (1986).
[9] H. Hattori, Y. Hikosaka, T. Hikida, and K. Mitsuke, J. Chem. Phys. **106**, 4902 (1997).
[10] S. T. Pratt, P. M. Dehmer, and J. L. Dehmer, J. Chem. Phys. **99**, 6233 (1993).
[11] R. Renner, Z. Phys. **92**, 172 (1934).
[12] J. A. Pople, Mol. Phys. **3**, 16 (1960).
[13] J. T. Hougen, J. Chem. Phys. **36**, 519 (1962).
[14] T. Barrow, R. N. Dixon, and G. Duxbury, Mol. Phys. **27**, 1217 (1974).
[15] Ch. Jungen and A. J. Merer, Mol. Phys. **40**, 1 (1980).
[16] J. M. Brown, J. Mol. Spectrosc. **68**, 412 (1977).
[17] R. N. Dixon, Philos. Trans. R. Soc. London, Ser. A **252**, 165 (1960).
[18] L. Gausset, G. Herzberg, A. Lagerqvist, and B. Rosen, Astrophys. J. **142**, 45 (1965).
[19] J. W. C. Johns, Can. J. Phys. **39**, 1738 (1961).
[20] H. W. Kroto, Can. J. Phys. **45**, 1439 (1967).
[21] K. Dressler and D. A. Ramsay, Philos. Trans. R. Soc. London, Ser. A **251**, 69 (1959).
[22] A. N. Petelin and A. A. Kiselev, Int. J. Quantum Chem. **6**, 701 (1972).
[23] M. Perić and S. D. Peyerimhoff, J. Chem. Phys. **102**, 3685 (1995).
[24] M. Perić, H. Thümmel, C. M. Marian, and S. D. Peyerimhoff, J. Chem. Phys. **102**, 7142 (1995).
[25] M. Perić, B. Ostojić, and B. Engels, J. Chem. Phys. **109**, 3086 (1998).
[26] M. Perić, B. Ostojić, and J. Radić-Perić, Phys. Rep. **290**, 283 (1997).
[27] J. Tang and S. Saito, J. Chem. Phys. **105**, 8020 (1996).
[28] S.-G. He and D. J. Clouthier, J. Chem. Phys. **120**, 8544 (2004) and references therein.
[29] S.-G. He and D. J. Clouthier, J. Chem. Phys. **123**, 014317 (2005).
[30] D. A. Hostutler, S.-G. He, and D. J. Clouthier, J. Chem. Phys. **121**, 5801 (2004).
[31] M. Li and J. A. Coxon, J. Mol. Spectrosc. **196**, 14 (1999).
[32] R. Colin, M. Herman, and I. Kopp, Mol. Phys. **37**, 1397 (1979).
[33] M. Herman and R. Colin, Phys. Scr. **25**, 275 (1982).
[34] V. Blanchet, S. Boyé, S. Zamith, A. Campos, B. Girard, J. Liévin, and D. Gauyacq, J. Chem. Phys. **119**, 3751 (2003).
[35] M. Takahashi, M. Fujii, and M. Ito, J. Chem. Phys. **96**, 6486 (1992).
[36] K. Müller-Dethlefs, M. Sander, and E. W. Schlag, Chem. Phys. Lett. **112**, 291 (1984).
[37] K. Müller-Dethlefs and E. W. Schlag, Annu. Rev. Phys. Chem. **42**, 109 (1991).
[38] J. C. Van Craen, M. Herman, R. Colin, and J. K. G. Watson, J. Mol. Spectrosc. **111**, 185 (1985).
[39] A. J. Merer, N. Yamakita, S. Tsuchiya, J. F. Stanton, Z. Duan, and R. W. Field, Mol. Phys. **101**, 663 (2003).
[40] R. Lindner, H.-J. Dietrich, and K. Müller-Dethlefs, Chem. Phys. Lett. **228**, 417 (1994).
[41] A. D. Buckingham, B. J. Orr, and J. M. Sichel, Philos. Trans. R. Soc. London, Ser. A **268**, 147 (1970).
[42] R. N. Dixon, G. Duxbury, M. Horani, and J. Rostas, Mol. Phys. **22**, 977 (1971).
[43] R. N. Dixon, G. Duxbury, J. W. Rababais, and L. Åsbrink, Mol. Phys. **31**, 423 (1976).
[44] S. N. Dixit and V. McKoy, Chem. Phys. Lett. **128**, 49 (1986).
[45] J. Xie and R. N. Zare, J. Chem. Phys. **93**, 3053 (1990).
[46] R. Signorell and F. Merkt, Mol. Phys. **92**, 793 (1997).
[47] C. K. Ingold and G. W. King, J. Chem. Soc. **1953**, 2702.
[48] K. K. Innes, J. Chem. Phys. **22**, 863 (1954).
[49] J. K. G. Watson, M. Herman, J. C. Van Craen, and R. Colin, J. Mol. Spectrosc. **95**, 101 (1982).
[50] V. H. Dibeler, J. A. Walker, and K. E. McCulloh, J. Chem. Phys. **99**, 2264 (1973).
[51] P. M. Dehmer and J. L. Dehmer, J. Electron. Spectrosc. Relat. Phenom. **28**, 145 (1982).
[52] Y. Ono, E. A. Osuch, and C. Y. Ng, J. Chem. Phys. **76**, 3905 (1982).
[53] W. A. Chupka, J. Chem. Phys. **96**, 4520 (1993).
[54] T. F. Gallagher, *Rydberg Molecules* (Cambridge University Press, Cambridge, 1994).
[55] F. Merkt, Annu. Rev. Phys. Chem. **48**, 675 (1997).
[56] K. Müller-Dethlefs, E. W. Schlag, E. R. Grant, K. Wang, and B. V. McKoy, Adv. Chem. Phys. **90**, 1 (1995), and references therein.
[57] Ch. Jungen and A. J. Merer, in *Molecular Spectroscopy*, Modern Research Vol. 2 edited by K. N. Rao and C. W. Mathews (Academic, New York, 1976), p. 127.
[58] G. Duxbury, B. D. McDonald, and A. Alijah, Mol. Phys. **89**, 767 (1996).
[59] J. M. Brown and F. Jørgensen, Annu. Rev. Phys. Chem. **52**, 117 (1983).
[60] J. M. Brown, in *Computational Molecular Spectroscopy*, edited by P. Jensen and P. R. Bunker (Wiley, New York, 2000), Chap. 16.
[61] D. Gauyacq and Ch. Jungen, Mol. Phys. **41**, 383 (1980).
[62] J. Plíva, J. Mol. Spectrosc. **44**, 165 (1972).
[63] I. M. Mills and A. G. Robiette, Mol. Phys. **56**, 743 (1985).
[64] M. S. Child and L. Halonen, Adv. Chem. Phys. **57**, 1 (1984).
[65] See EPAPS Document No. E-JCPSA6-124-004619 for six pages of tabular material containing the assigned rotational lines and their residuals (doc format). This document can be reached via a direct link in the online article's HTML reference section or via the EPAPS homepage (http://www.aip.org/pubservs/epaps.html).
[66] Y. Kabbadj, M. Herman, G. Di Lonardo, L. Fusina, and J. W. C. Johns, J. Mol. Spectrosc. **150**, 535 (1991).
[67] T. J. Lee, J. E. Rice, and H. F. Schaefer III, J. Chem. Phys. **86**, 3051 (1987).
[68] Y. F. Zhu, R. Shehadeh, and E. R. Grant, J. Chem. Phys. **99**, 5723 (1993).
[69] J. H. Fillion, A. Campos, J. Pedersen, N. Shafizadeh, and D. Gauyacq, J. Chem. Phys. **105**, 22 (1996).
[70] M. N. R. Ashfold, B. Tutcher, B. Yang, Z. K. Jin, and S. L. Anderson, J. Chem. Phys. **87**, 5105 (1987).
[71] C. Cha, R. Weinkauf, and U. Boesl, J. Chem. Phys. **103**, 5224 (1995).